Nonaxisymmetric Instabilities in Massive, Self-gravitating Disks

James N. Imamura
Institute of Theoretical Science
University of Oregon

Star formation occurs in Giant Molecular Clouds where cold condensed cores collapse triggered by external mechanisms, such as shock waves or stellar winds. For initially static cores, collapse is spherically symmetric and solar-type stars form on timescales of tens of millions of years. Observations, however, have shown that typical cloud cores have large specific angular momenta ~ 10^{21} cm^2/s. The specific angular momenta of cloud cores are too high to allow collapse directly to a star, only a few percent of the matter falls into the central object for typical low-mass cores, the rest settles into a disk. Star formation thus hinges on the question of how the disk material accretes onto the central object and thus requires knowledge of viscosity in the disk. Ordinary molecular viscosity cannot supply the dissipation; nonaxisymmetric hydrodynamic and/or magnetohydrodynamic instabilities are often invoked to supply the transport directly or to generate turbulence and so enhance the viscosity. We investigate the hydrodynamic stability properties of massive, self-gravitating disks to study this question. We model disks in the linear, quasi-linear, and nonlinear regimes with a goal of elucidating the general nature of global, nonaxisymmetric disk instabilities by mapping the regimes of instability in the relevant parameter space, and then developing a quasi-linear theory to model the evolution of linearly unstable disks into the nonlinear regime.

Nonaxisymmetric Instabilities in Massive, Self-gravitating Disks

I. Physical Problem
II. Nonaxisymmetric Disk Modes and Disk Instability Regimes
III. Mass and Angular Momentum Transport: Quasi-linear Theory and Nonlinear Simulations
IV. Summary and Future Directions

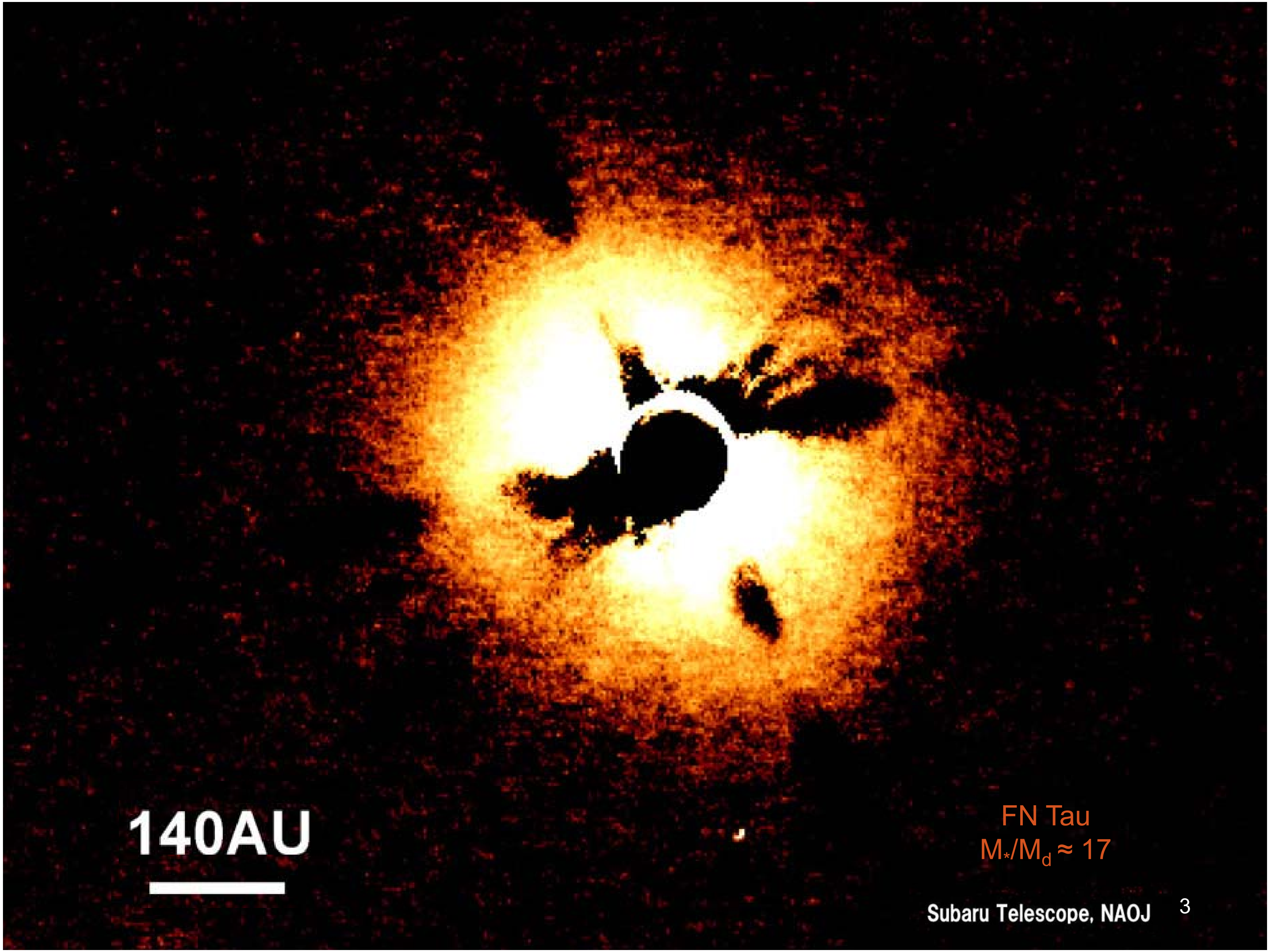

140AU
FN Tau
$M_*/M_d \approx 17$
Subaru Telescope, NAOJ

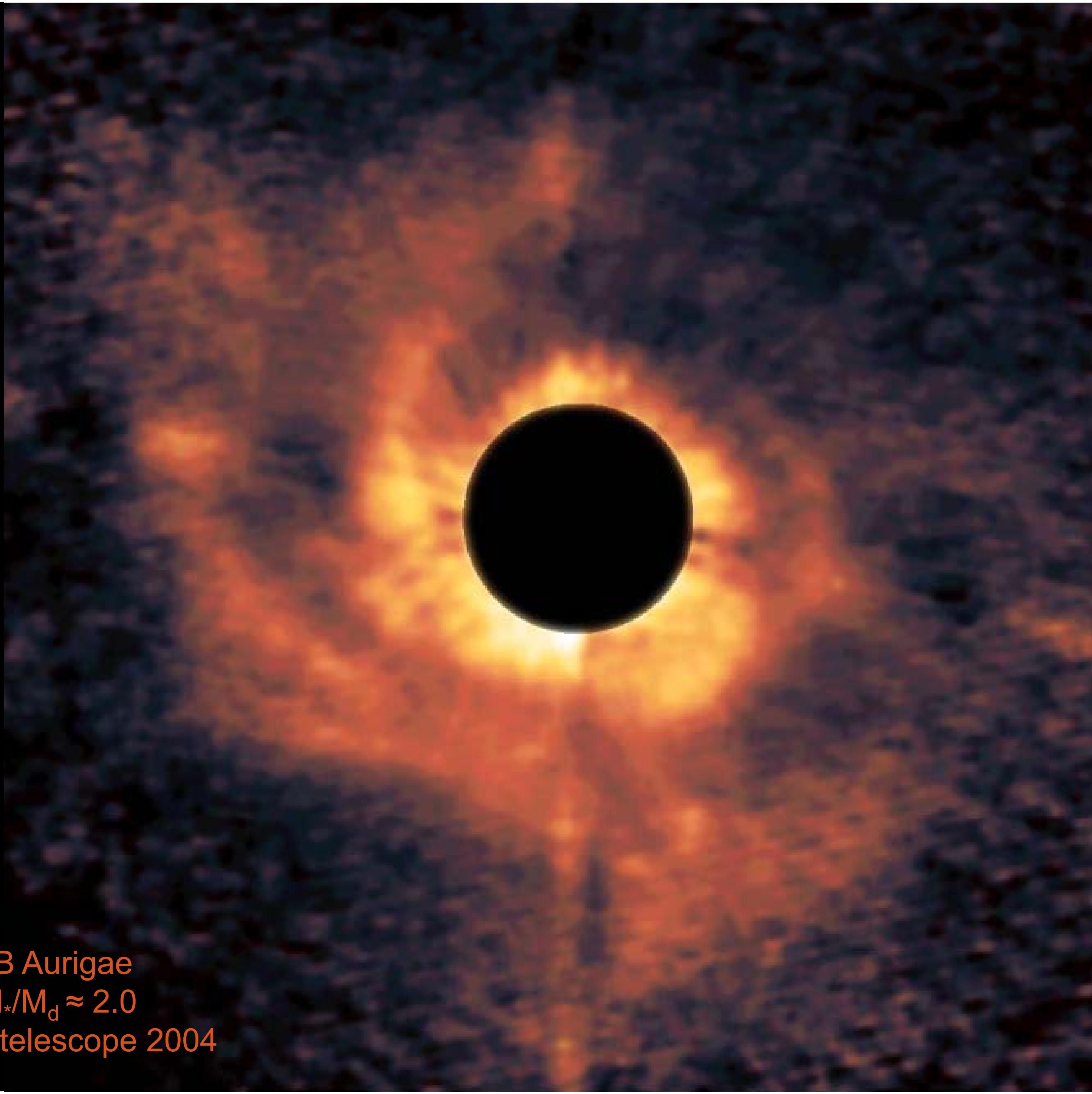

AB Aurigae

$M_*/M_d \approx 2.0$

Subaru telescope 2004

I. Physical Problem: Disk formation

- Clouds with high specific angular momenta ~ 10^{21} cm^2/s , spin up and flatten as they collapse
- Material near the spin axis has little angular momentum and so falls inward, forming a central object with a few percent of the mass of the cloud. The rest of the cloud settles into a massive circumstellar disk (e.g., Kratter *et al*. 2011)
- In our Solar System , the Sun contains over 99% of the total mass of the system
- Some mechanism must have caused the matter of the disk to flow inward
- We model disks with a wide range of properties to analyze the nature of nonaxisymmetric disk modes and define instability regimes in the relevant parameter space. We address the question of angular momentum transport.

http://www.spitzer.caltech.edu/images

II. Nonaxisymmetric Instabilities in Disks

- Previous studies (plus many other unmentioned ones)
  - Papaloizou & Pringle (1984, 1987)
    - Slender annuli and rings
  - Goldreich, Goodman & Narayan (1986)
    - Slender, incompressible tori
    - Thin ribbon approximation
  - Kojima (1986, 1989)
    - Non-self-gravitating disks
  - Adams, Ruden & Shu (1989), Heemskerk *et al.* (1992), Noh, Vishniac & Cochran (1992), Taga & Iye (1998)
    - m=1 mode, central star motion, thin disks
  - Andalib, Tohline & Christodoulou (1998)
    - Slender incompressible tori (ICTs)
  - Hachisu & Tohline (1992), Woodward, Tohline & Hachisu (1994)
    - Nonlinear study of self-gravitating disks
  - Shariff (2009)
    - Review of current work, observation
    - Magnetic effects, radiation transport

Nonaxisymmetric Disk Instabilities (cont'd)

- Our (students and Imamura) work (Hadley & Imamura 2009,2011, Hadley *et al*. 2011a,b)
  - Build an extensive library of equilibrium disks and map *linear* instability regimes
    - ~7700 equilibrium disks
    - ~2100 time evolved models
  - Find and analyze trends
    - Build parameter space maps
      - Location of modal types
      - Instability mechanisms
  - Mass and Angular momentum transport, *quasi-linear* theory and *nonlinear* simulations
  - Comparison of quasi-linear and nonlinear works

Numerical Modeling of Disks: Hydrodynamic Equations

$$\frac{\partial}{\partial t}\rho + \nabla \cdot (\rho v) = 0,$$

Continuity Equation

$$\frac{\partial}{\partial t}\rho v + \nabla \cdot (\rho v v) + \nabla (P + P_Q) + \rho \nabla \Phi_g = 0,$$

Momentum Conservation

$$\frac{\partial}{\partial t}\varepsilon^{1/\gamma} + \nabla \cdot \varepsilon^{1/\gamma} v - \frac{\varepsilon^{1/\gamma - 1}}{\gamma}\Gamma_Q = 0,$$

Internal Energy Conservation

$$\nabla^2 \Phi_g - 4\pi G \rho = 0$$

Poisson Equation

where ρ is the mass density, v is the flow velocity, P is the pressure, Φ_g is the gravitational potential, ε is the internal energy, γ is the adiabatic gamma, t is the time, P_Q and Γ_Q are artificial viscosity parameters (Hawley 1984) and G is the gravitational constant.

Equilibrium modeling of disks

- Solve time independent hydrodynamic equations without artificial viscosity for the equilibrium solution using the self-consistent field approach (Hachisu 1986).
    - Assumptions:
        - constant entropy; polytropic relation for pressure and density
        - axisymmetry and power law rotation on cylinders
        - mirror symmetry across equatorial plane
- The hydrodynamic equations are normalized such that K = G = M = 1 (*polytrope* units) and we use cylindrical coordinates,

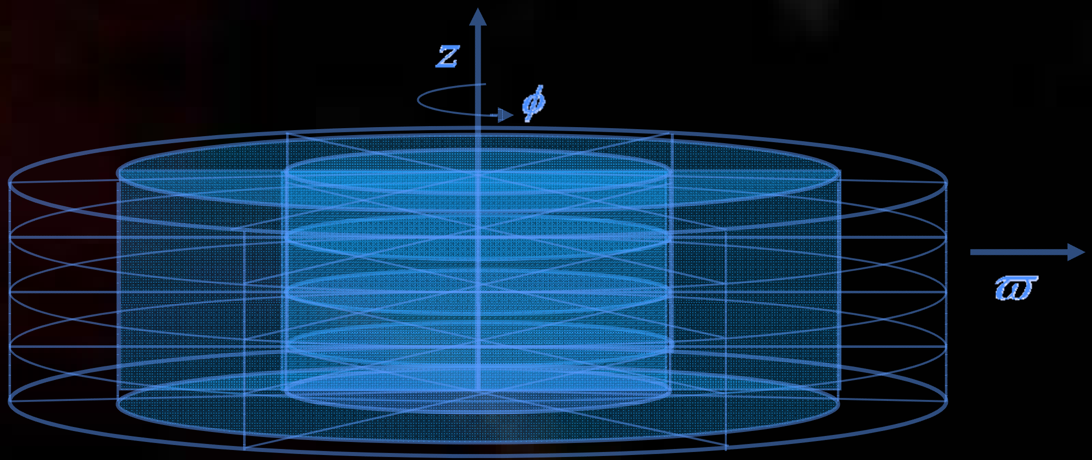

ϖ is the radial coordinate, ϕ is the azimuthal coordinate, and z is the vertical coordinate. The rotation axis is parallel to the z-axis.

Equilibrium Models

- Large r_-/r_+
  - Approach circular cross-section
    - Narrow disk approximation (ICT)
- Small r_-/r_+
  - ρ_0 moves inward, toward star and opposite side of the disk
  - ρ_0 increases, increasing pressure, disk puffs up

- Large M_*/M_d
  - Offsets ρ_0 toward the star

- Power law rotation

$$\Omega = \Omega_0 \left(\frac{\varpi}{R_0} \right)^{-q}$$

  - q = 2.0
    - Disks are axisymmetrically unstable when specific angular momentum decreases outward, q = 2.0 is bounding case
  - q = 1.5
    - Keplerian rotation
    - Higher velocity as r increases than q = 2.0
      - More centrifugal support
      - ρ_0 not offset, disks tend to flatten out

Equilibrium mass density contours

q = 2.0

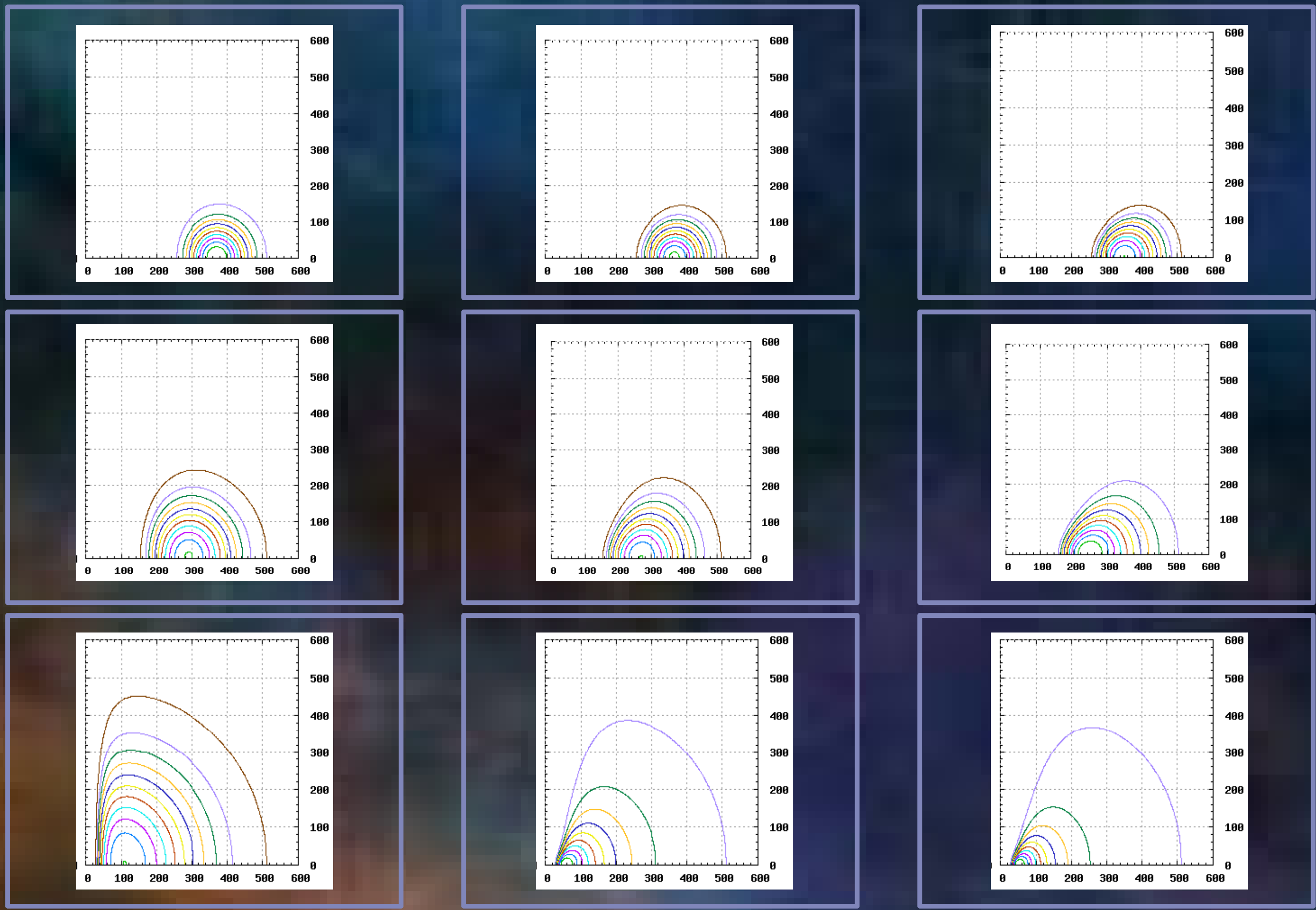

$r_-/r_+ = .50$

$r_-/r_+ = .30$

$r_-/r_+ = .10$

$M_*/M_d = 0.0$ $M_*/M_d = 1.0$ $M_*/M_d = 10.0$

Equilibrium mass density contours

$q = 1.75$

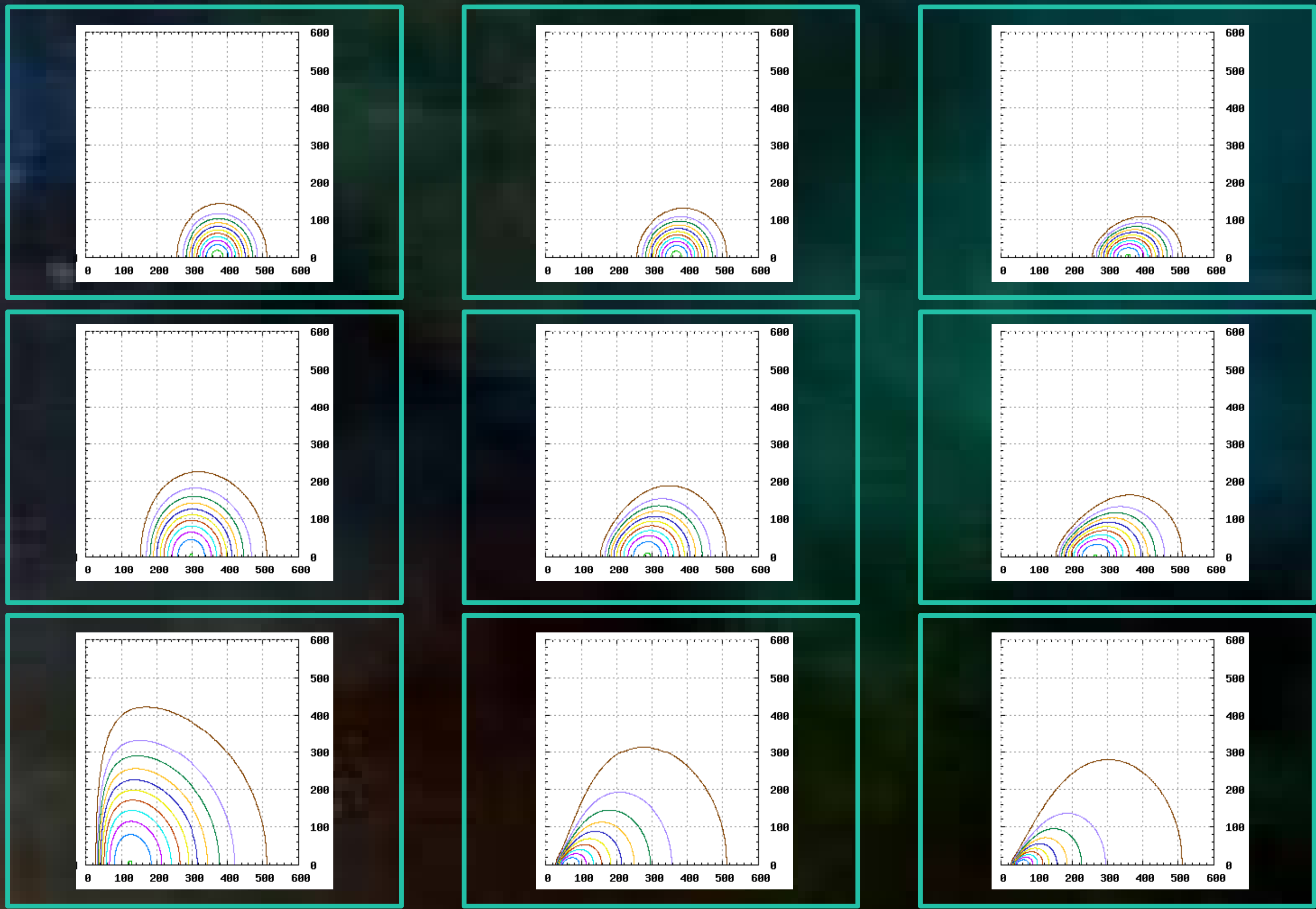

$r_-/r_+ = .50$

$r_-/r_+ = .30$

$r_-/r_+ = .10$

$M_*/M_d = 0.0$ $M_*/M_d = 1.0$ $M_*/M_d = 10.0$

Equilibrium mass density contours

$q = 1.5$

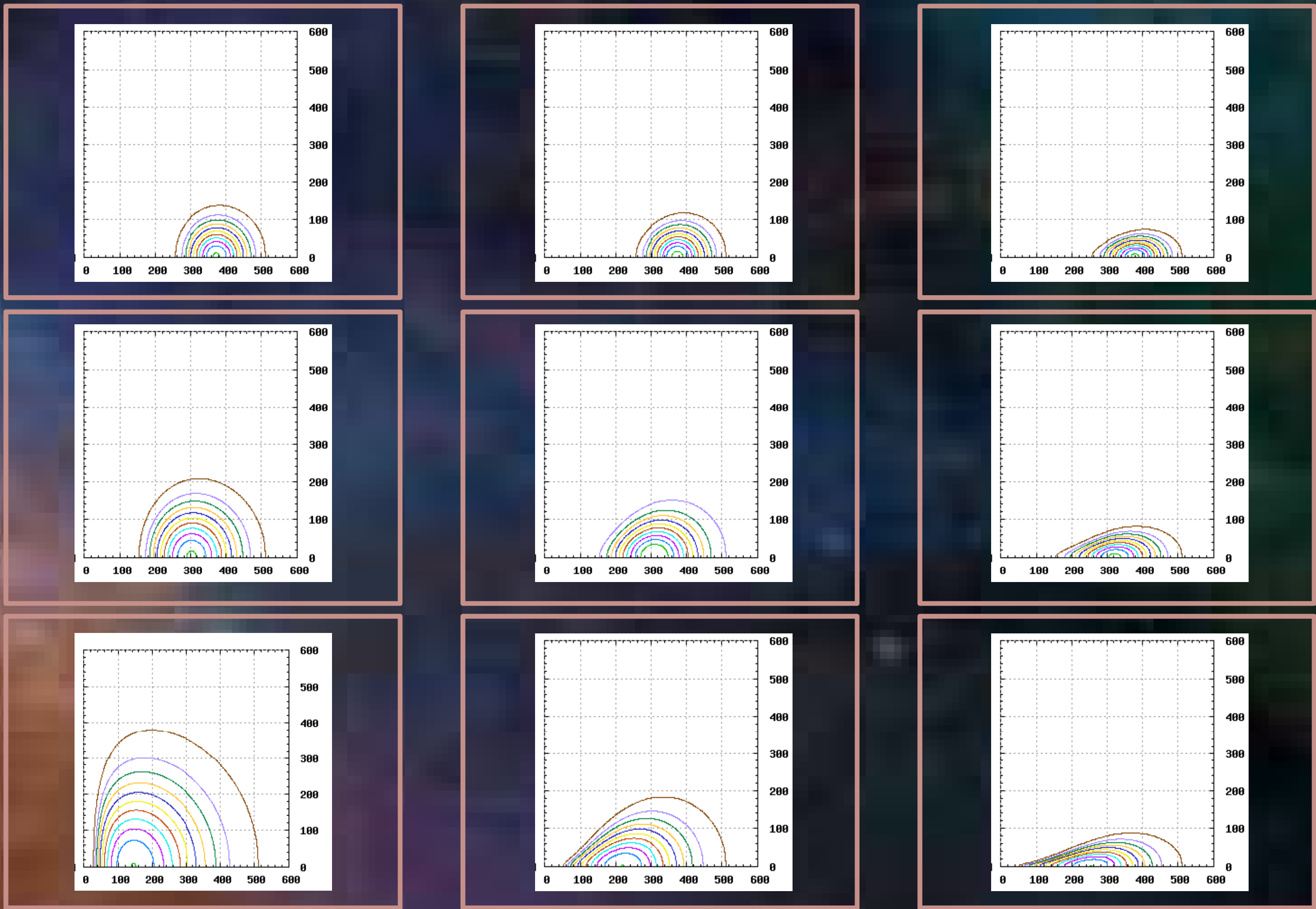

$r_-/r_+ = .50$

$r_-/r_+ = .30$

$r_-/r_+ = .10$

$M_*/M_d = 0.0$ $M_*/M_d = 1.0$ $M_*/M_d = 10.0$

Linear Stability Analysis

- Solve linearized time dependent hydrodynamic equations without artificial viscosity using the equilibrium solution as the background flow
    - Assumptions:
        - constant entropy; polytropic equation-of-state
        - mirror symmetry across equatorial plane
- The linearized hydrodynamic equations are found using Eulerian perturbations (see below and next slide).
- Perturbed variables

mass density $\rightarrow \rho = \rho_\circ(\varpi, z) + \delta\rho(\varpi, z, t)e^{im\phi}$

fluid velocity $\rightarrow \vec{v} = \vec{v_\circ}(\varpi, z) + \delta\vec{v}(\varpi, z, t)e^{im\phi}$

$$v_\varpi = \delta v_\varpi(\varpi, z, t)e^{im\varphi}$$

$$v_\phi = \Omega\varpi + \delta v_\phi(\varpi, z, t)e^{im\phi}$$

$$v_z = \delta v_z(\varpi, z, t)e^{im\phi}$$

pressure $\rightarrow P = P_\circ + \delta P(\varpi, z, t)e^{im\phi}$

gravitational potential $\rightarrow \Phi_g = \Phi_\circ + \delta\Phi_g(\varpi, z, t)e^{im\phi}$

Linear Evolution Equations (Initial Value Problem)

$$\partial_t \delta\rho = -im\Omega\delta\rho - \frac{1}{\varpi}\rho_0\delta v_\varpi - \delta v_\varpi \partial_\varpi \rho_0 - \delta v_z \partial_z \rho_0$$
$$- \rho_0\left(\partial_\varpi \delta v_\varpi + \frac{im}{\varpi}\delta v_\phi + \partial_z \delta v_z\right)$$

$$\partial_t \delta v_\varpi = -im\Omega\delta v_\varpi + 2\Omega\delta v_\phi - \gamma\frac{P_0}{\rho_0^2}\partial_\varpi \delta\rho$$
$$-(\gamma-2)\frac{\delta\rho}{\rho_0^2}\partial_\varpi P_0 - \partial_\varpi \delta\Phi$$

$$\partial_t \delta v_\phi = -im\Omega\delta v_\phi - \frac{1}{\varpi}\partial_\varpi\left(\Omega\varpi^2\right)\delta v_\varpi - \frac{im}{\varpi}\frac{P_0}{\rho_0^2}\delta\rho - \frac{im}{\varpi}\delta\Phi$$

$$\partial_t \delta v_z = -im\Omega\delta v_z - \gamma\frac{P_0}{\rho_0^2}\partial_z \delta\rho - (\gamma-2)\frac{\delta\rho}{\rho_0^2}\partial_z P_0 - \partial_z \delta\Phi$$

Initial Value Solver

- Solve linearized hydrodynamic equations by discretizing spatial derivaitves, but leaving the time derivatives continuous (Mehtod of Lines)
- The simulation is seeded with random, low-amplitude noise and the solutions advanced in time using a fourth-order Runge-Kutta scheme.
- Parameters:
    - Power law index of angular velocity distriibution, q
    - Star mass / disk mass ratio
    - Inner disk radius / outer disk radius ratio
    - Azimuthal mode number, m
- Analyze models for stability and modal characteristics

m = 2, *q* = 1.5, *r-/r+* = 0.30, M_*/M_d = 0.0

$|\delta\rho|/\rho_0$

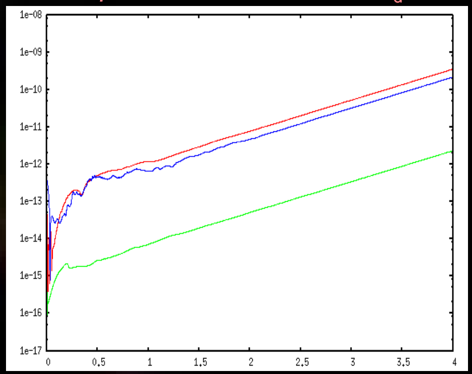

Time (MIRP)

m = 2, *q* = 1.5, *r-/r+* = 0.10, M_*/M_d = 0.1

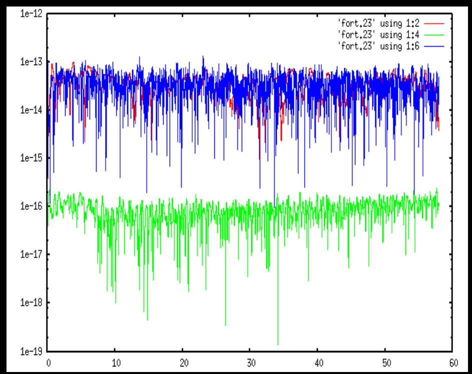

Time (MIRP)

Growth Rates and Oscillation Frequencies: Self-gravitating Toroids

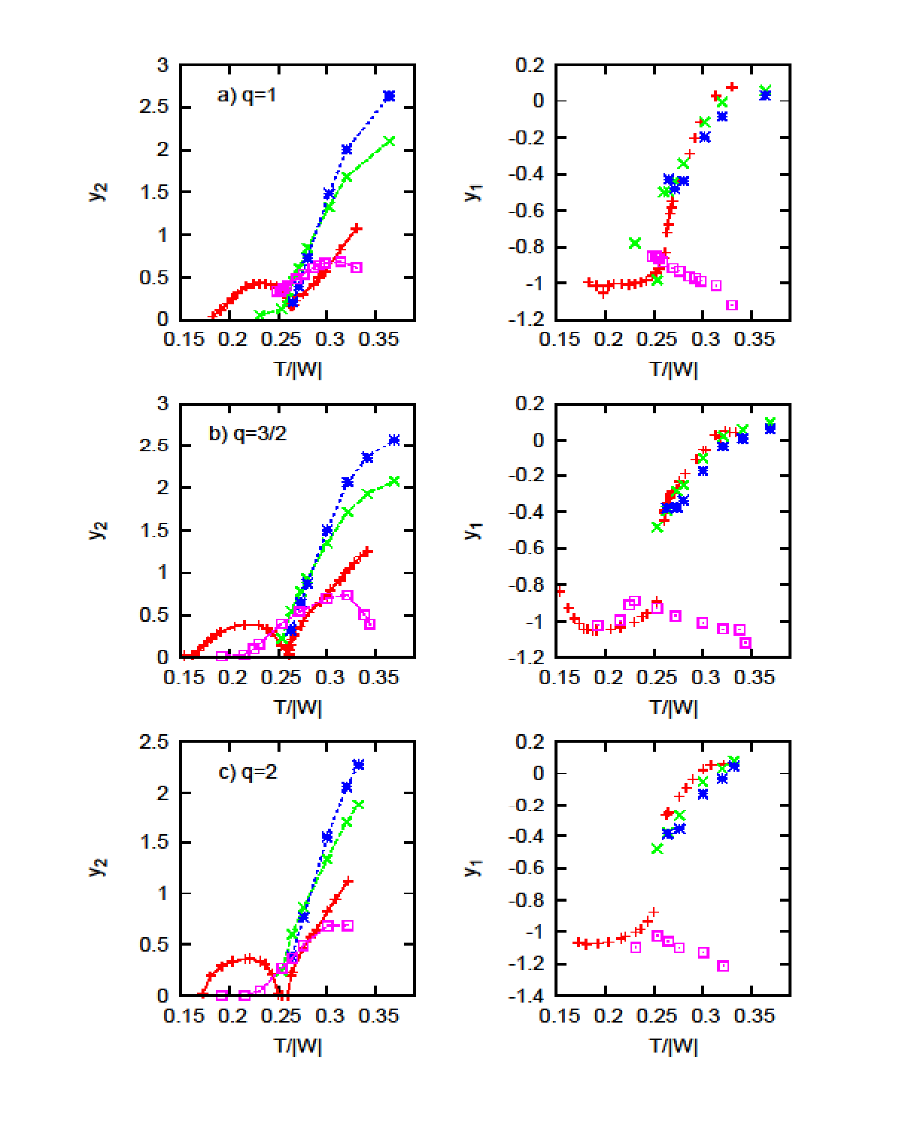

Toroid eigenvalues:

$$y_1 = \frac{\omega_{m,R}}{m} - \Omega_m, \text{ and } y_2 = \frac{\omega_{m,I}}{\Omega_m},$$

where $\omega_{m,R}$ and $\varpi_{m,I}$ are the real and imaginary parts of the eigenvalue, and Ω_m is the angular frequency at the location of the maximum density in the disk.

The q-values are the exponents of the power law $\Omega(\varpi)$. The m =1,2,3,4 eigenvalues are in magenta, red, green, and blue, respectively. At low T/|W|, I modes dominate. At high T/|W|, J modes dominate. These general results hold for star/disk systems as well.

Mode types

Equilibrium mass density contours

I^+

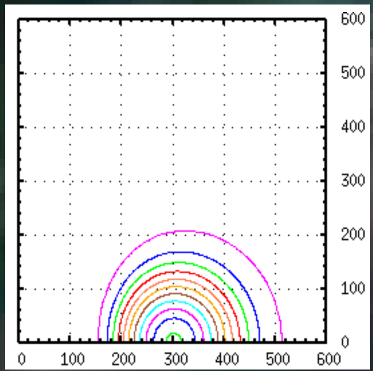

$q = 1.5$, $r_-/r_+ = 0.30$ $M_*/M_d = 0.0$

I^-

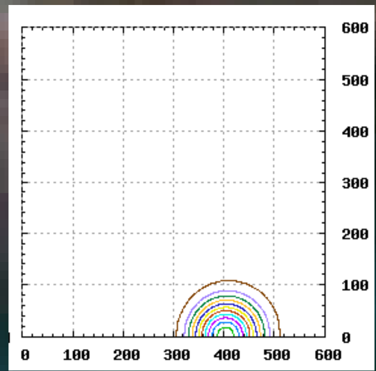

$q = 1.5$, $r_-/r_+ = 0.60$ $M_*/M_d = 0.1$

J

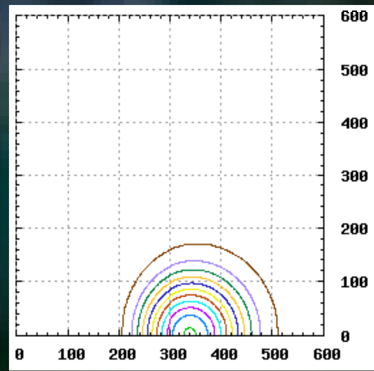

$q = 1.5$, $r_-/r_+ = 0.40$ $M_*/M_d = 0.0$

P

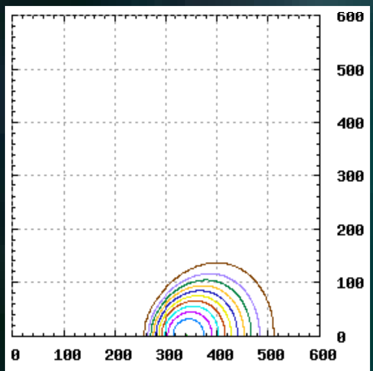

$q = 2.0$, $r_-/r_+ = 0.50$ $M_*/M_d = 100.0$

Edge

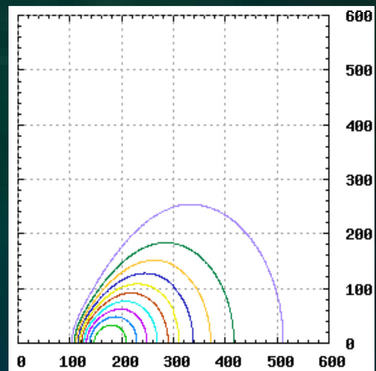

$q = 2.0$, $r_-/r_+ = 0.20$ $M_*/M_d = 100.0$

A

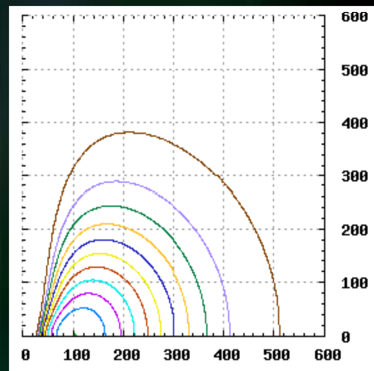

$q = 1.75$, $r_-/r_+ = 0.05$ $M_*/M_d = 0.1$

Mode types

Eigenfunction amplitudes $|\delta\rho|/\rho_0$

I^+

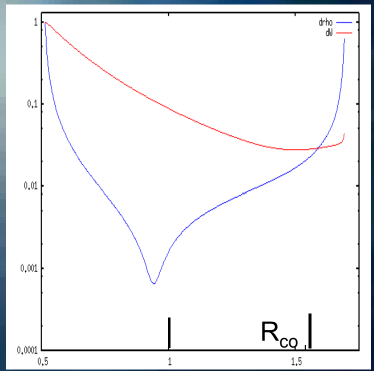

q = 1.5, r_-/r_+ = 0.30 M_*/M_d = 0.0

I^-

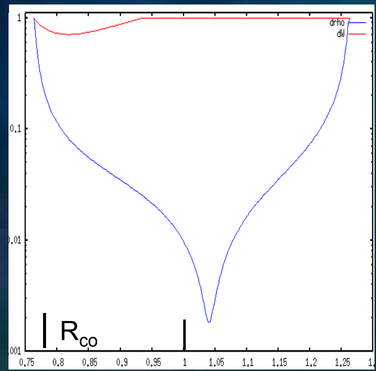

q = 1.5, r_-/r_+ = 0.60 M_*/M_d = 0.1

J

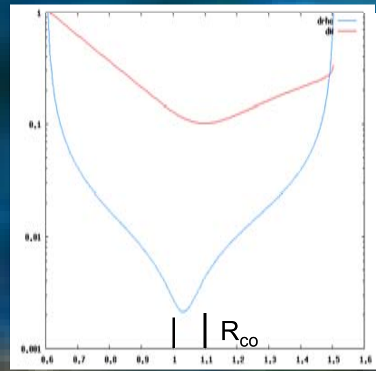

q = 1.5, r_-/r_+ = 0.40 M_*/M_d = 0.0

P

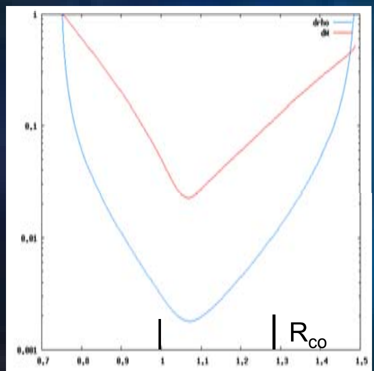

q = 2.0, r_-/r_+ = 0.50 M_*/M_d = 100.0

Edge

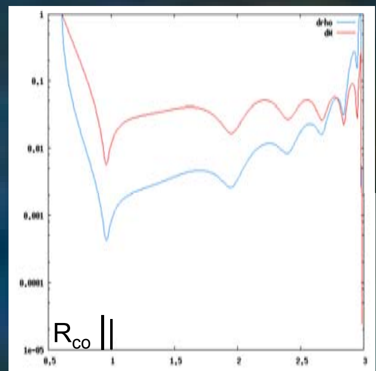

q = 2.0, r_-/r_+ = 0.20 M_*/M_d = 100.0

A

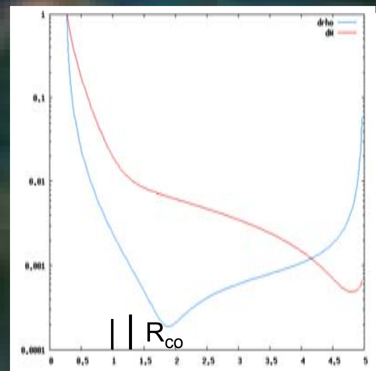

q = 1.75, r_-/r_+ = 0.05 M_*/M_d = 0.1

Mode types

Eigenfunction phases

I⁺

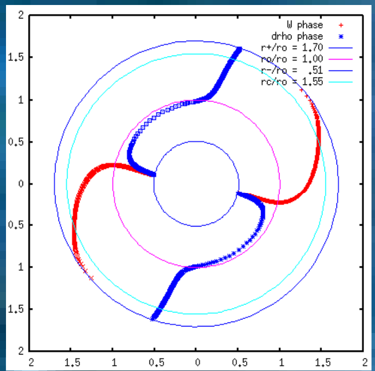

$q = 1.5$, $r_-/r_+ = 0.30$ $M_*/M_d = 0.0$

I⁻

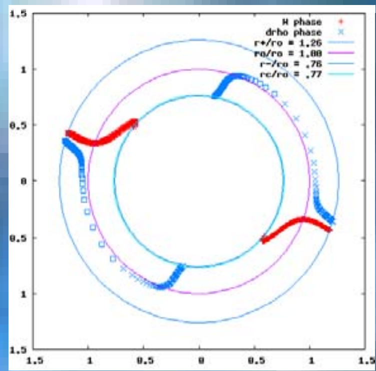

$q = 1.5$, $r_-/r_+ = 0.60$ $M_*/M_d = 0.1$

J

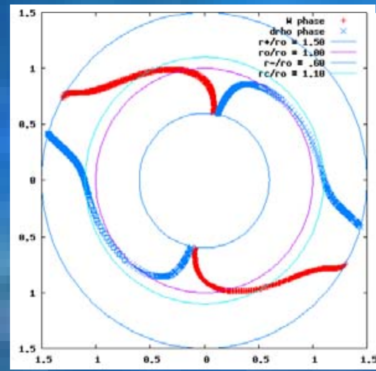

$q = 1.5$, $r_-/r_+ = 0.40$ $M_*/M_d = 0.0$

P

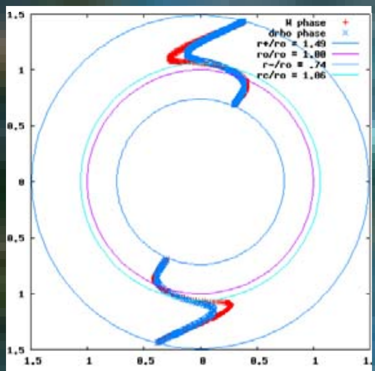

$q = 2.0$, $r_-/r_+ = 0.50$ $M_*/M_d = 100.0$

Edge

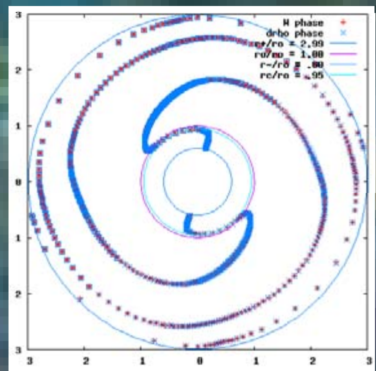

$q = 2.0$, $r_-/r_+ = 0.20$ $M_*/M_d = 100.0$

A

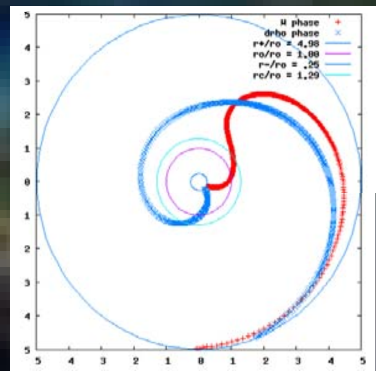

$q = 1.75$, $r_-/r_+ = 0.05$ $M_*/M_d = 0.1$

Mode types

Locations in parameter space

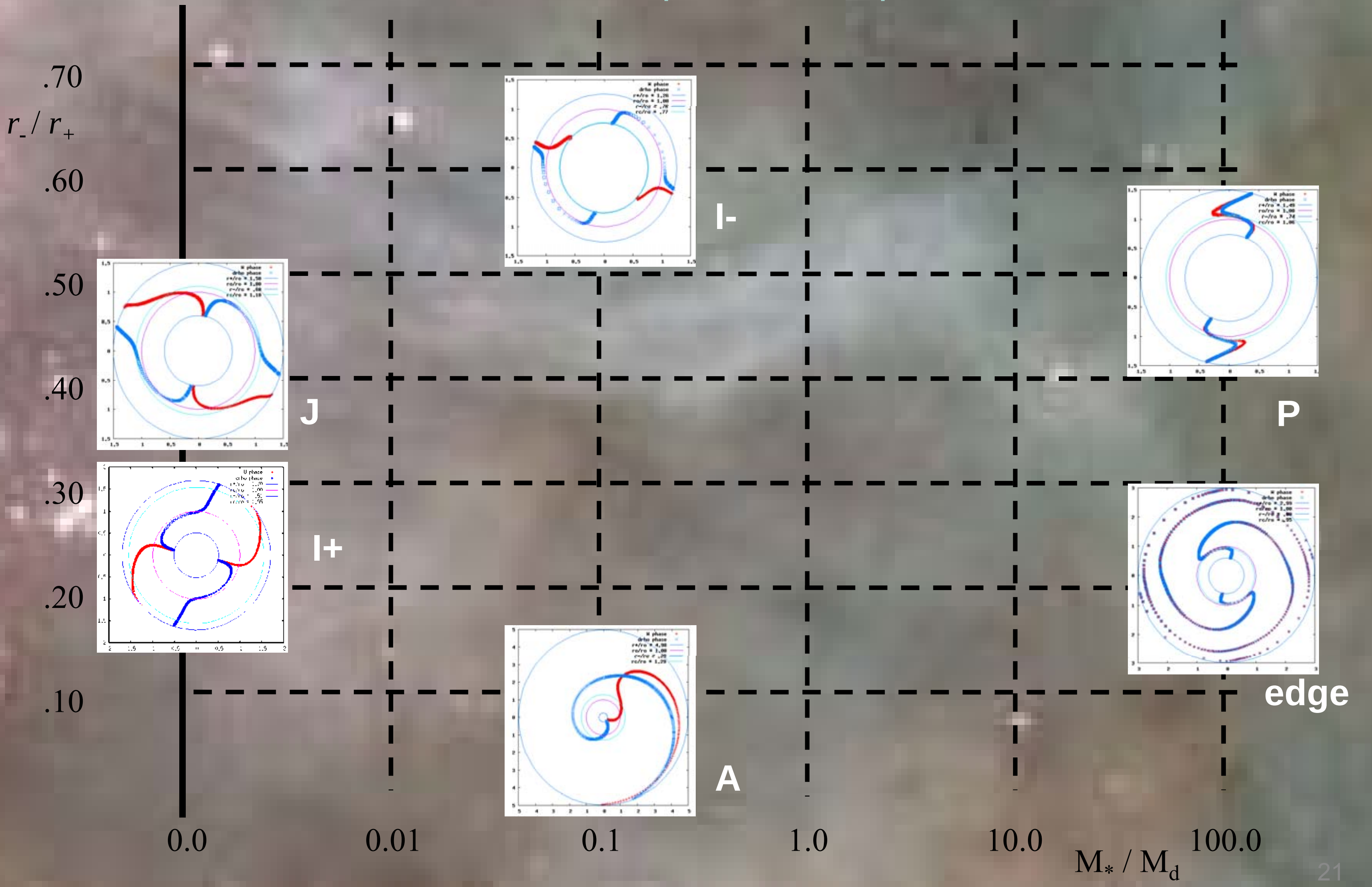

Mode types

Eigenfunction phases

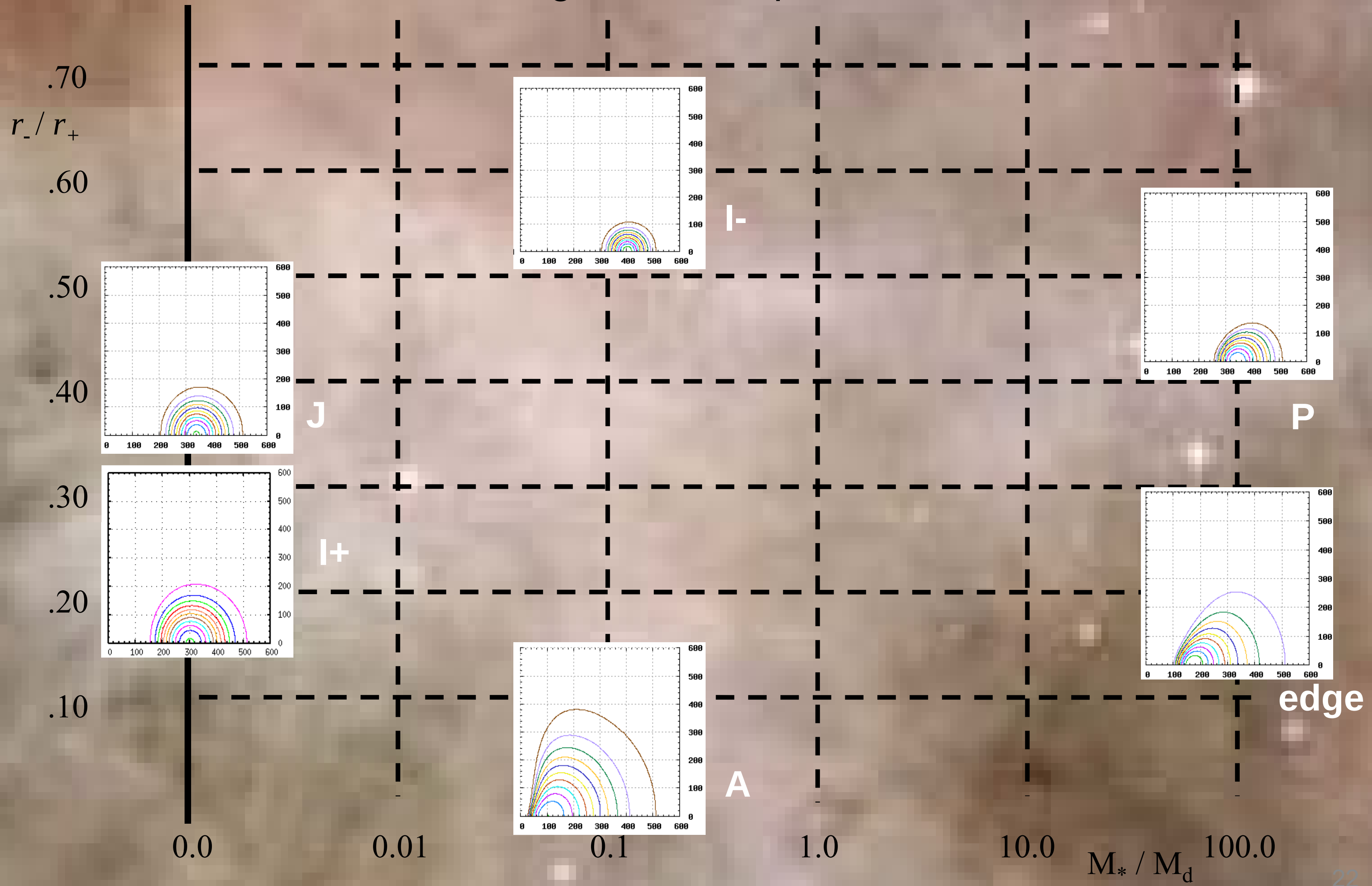

Work integrals and stresses

- Work integrals
  - Total energy carried by the perturbation is the sum of the work done by perturbed kinetic energy plus the work done by perturbed enthalpy

$$\langle E\rangle \equiv \frac{1}{2}\rho_0\left\langle \delta v_\varpi^2 + \delta v_\phi^2 + \delta v_z^2 \right\rangle + \frac{1}{2}\gamma\frac{P_0}{\rho_0^2}\left\langle \delta\rho^2 \right\rangle$$

- Stresses
  - Time derivative of energy is the sum of the stresses $\frac{d}{dt}\langle E\rangle = \sigma_R + \sigma_\Pi + \sigma_\Phi$
  - Reynolds stress measures the power arising from shear stress of the equilibrium structure affecting the perturbed model

$$\sigma_R \equiv -\rho_0\varpi\frac{\partial\Omega}{\partial\varpi}\left\langle \delta v_\varpi \delta v_\phi \right\rangle$$

  - Acoustic wave flux carried by the perturbation redistributes energy

$$\sigma_\Pi \equiv -\vec{\nabla}\cdot\left\langle \delta P \delta\vec{v} \right\rangle$$

  - Perturbed gravity contains input from the self-gravity of the disk as well as motion of the central star in the m = 1 case

$$\sigma_\Phi \equiv -\rho_0\left\langle \delta\vec{v}\cdot\vec{\nabla}\left(\delta\Phi_d + \delta\Phi_*\right)\right\rangle$$

Mode Energetics: Perturbed Energies

I^+

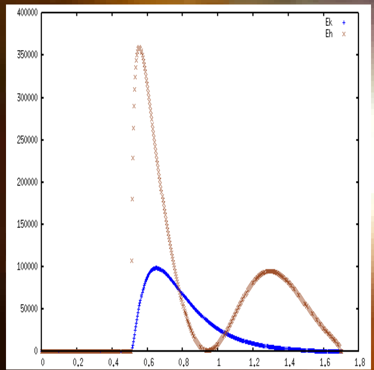

$q = 1.5$, $r_-/r_+ = 0.30$ $M_*/M_d = 0.0$

I^-

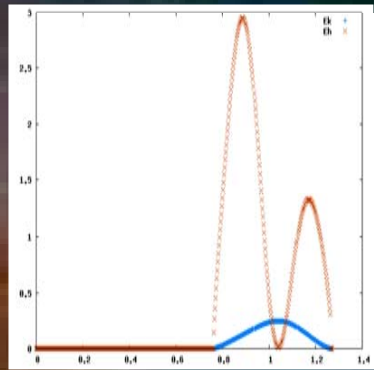

$q = 1.5$, $r_-/r_+ = 0.60$ $M_*/M_d = 0.1$

J

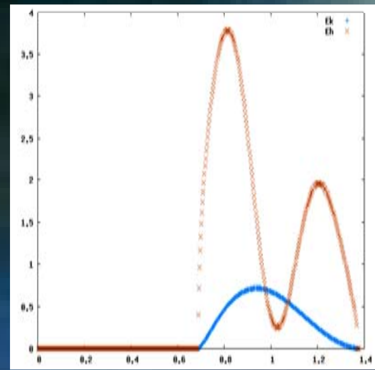

$q = 1.5$, $r_-/r_+ = 0.40$ $M_*/M_d = 0.0$

P

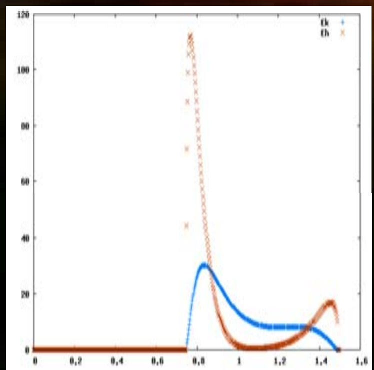

$q = 2.0$, $r_-/r_+ = 0.50$ $M_*/M_d = 100.0$

Edge

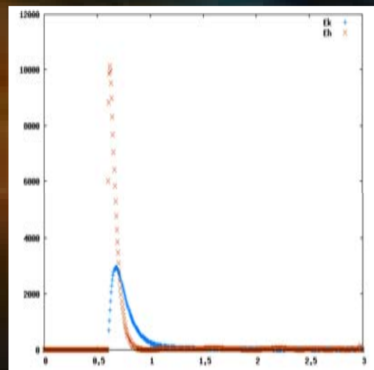

$q = 2.0$, $r_-/r_+ = 0.20$ $M_*/M_d = 100.0$

A

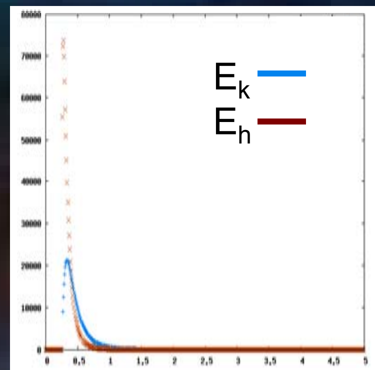

$q = 1.75$, $r_-/r_+ = 0.05$ $M_*/M_d = 0.1$

Mode Energetics: Stresses

I^+

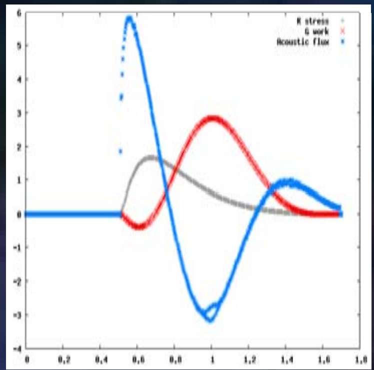

q = 1.5, $r_-/r_+ = 0.30$ $M_*/M_d = 0.0$

I^-

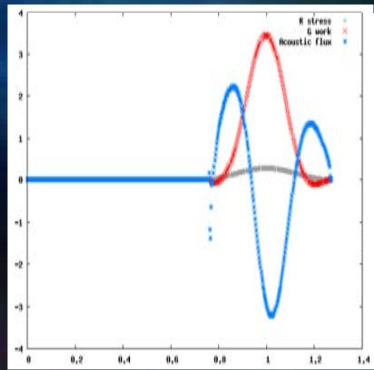

q = 1.5, $r_-/r_+ = 0.60$ $M_*/M_d = 0.1$

J

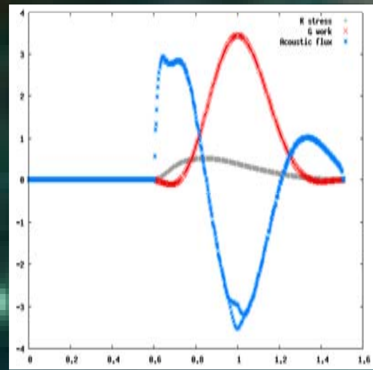

q = 1.5, $r_-/r_+ = 0.40$ $M_*/M_d = 0.0$

P

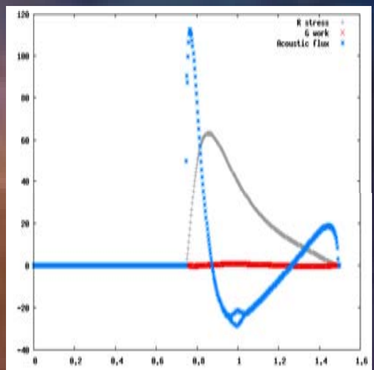

q = 2.0, $r_-/r_+ = 0.50$ $M_*/M_d = 100.0$

Edge

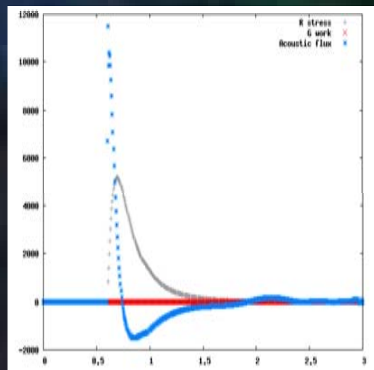

q = 2.0, $r_-/r_+ = 0.20$ $M_*/M_d = 100.0$

A

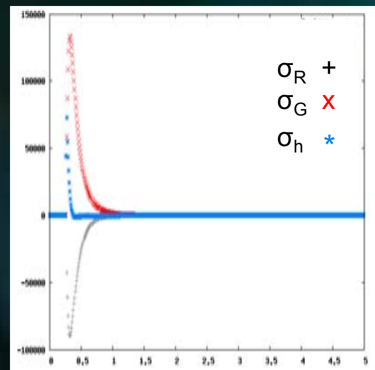

q = 1.75, $r_-/r_+ = 0.05$ $M_*/M_d = 0.1$

Parameter space map

q = 2.0, *m* = 2

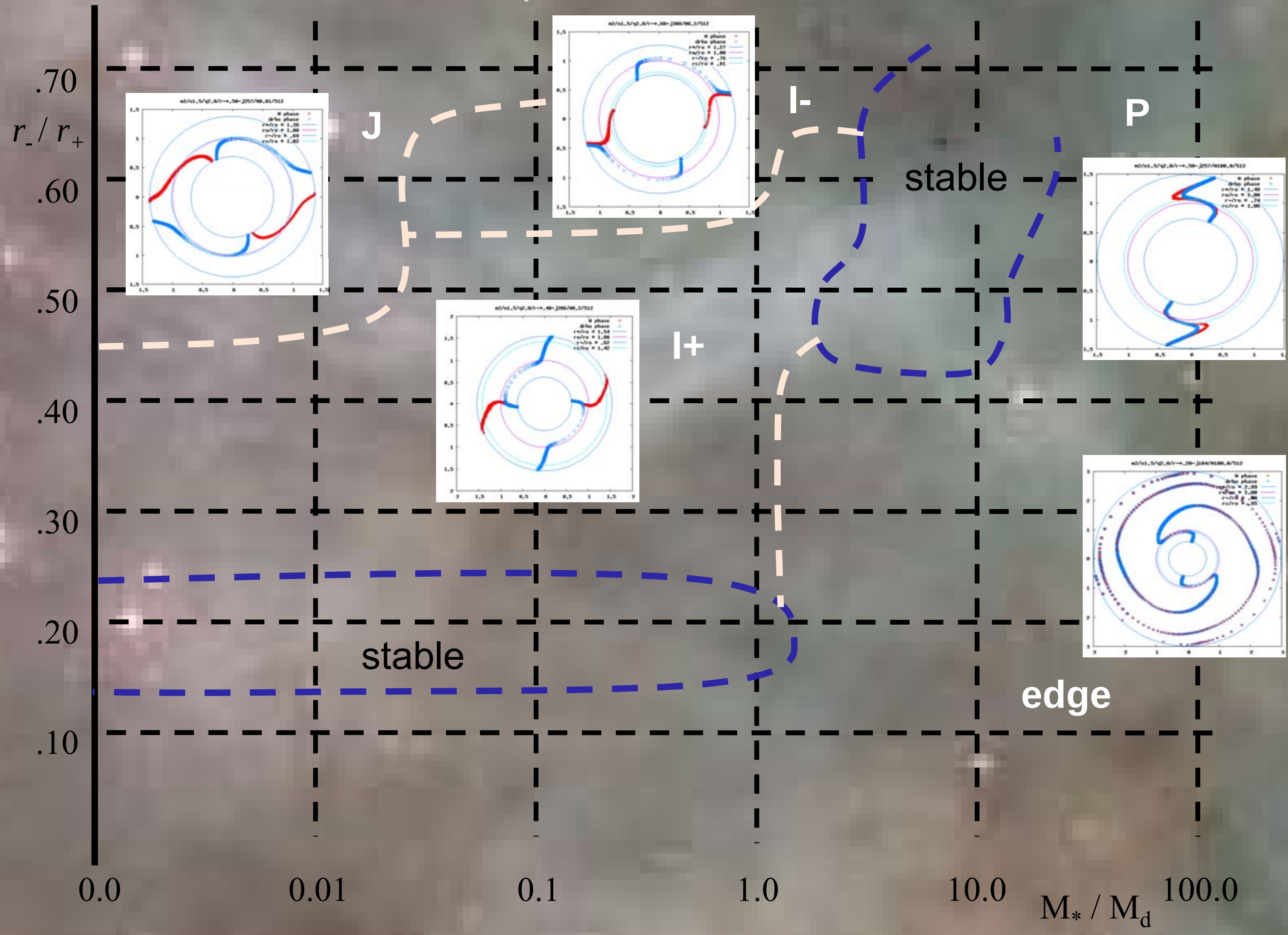

Parameter space map

q = 2.0, m = 2

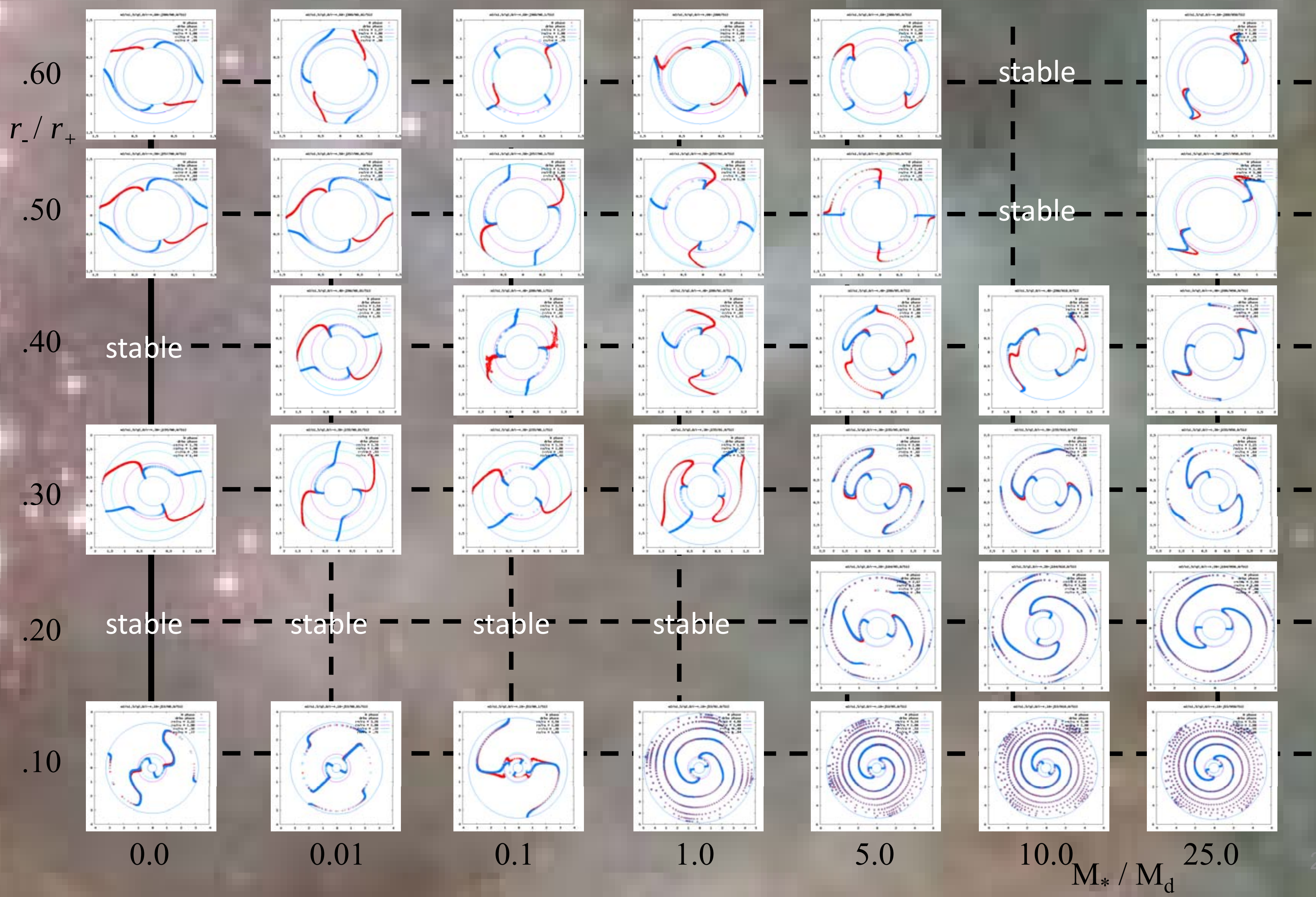

r/r_+	$q = 1.5$								
	M_*/M_d								
	0.0	0.01	0.1	1.0	5.0	10.0	25.0	50.0	100.0
0.65	4 3 2 1	4 3 2 1	4 3 2 1	2 3 4 1	4 2 1	4 2	3 4 2	4	stable
0.60	4 3 2 1	4 3 2 1	4 3 1 2	4 3 2 1	3 4 2 1	3 2 4	3 4 2	3 4 2	stable
0.55	4 3 2 1	4 3 2 1	4 3 1 2	4 3 2 1	3 2 4	2 3 4	4 3 2	3 4	stable
0.50	4 3 1 2	4 3 1 2	4 3 1 2	3 4 2 1	2 3 4 1	2 3 4	3 4 1	3 4 2	stable
0.45	3 4 1 2	3 4 1 2	4 1 2 3	3 2 4 1	2 3 4 1	2 3 4	2 3 4	stable	stable
0.40	3 4 1 2	3 4 1 2	2 1 3 4	2 3 1 4	2 3 4 1	2 3 4 1	3 4 2	stable	stable
0.35	1 3 4 2	1 3 2 4	2 3 1 4	2 1 3 4	2 3 1 4	2 3 4	2 3	stable	stable
0.30	2 1	2 1 3	2 1 3	1 2 3 4	2 1 3 4	2 3 4	3 2	stable	stable
0.25	2 1	2 1	2 1 3	1 2 3	2 1	2 3	stable	stable	stable
0.20	2 1	2 1	1 2	1 2 3	2 1	2	stable	stable	stable
0.15	2 1	1 2	1 2	1 2	2 1 3	2	stable	stable	stable
0.10	1	1	1	1	1 2	2	stable	stable	stable
0.05	1	1	1 2 3	1	1	2	stable	stable	stable

Table 4.2.1. Approximate modal dominance regimes for $q = 1.5$ for $m = 1, 2, 3$, and 4.

	$q = 2.0$								
0.65	4 3 2 1	4 3 2 1	4 3 2 1	4 2 3 1	4 3 2 1	3 4 1 2	1	1 3 2	2 3 1 4
0.60	4 3 2 1	4 3 2 1	4 3 1 2	3 4 2 1	3 2 4 1	1	1	1 2 4	2 1 4
0.55	4 3 2 1	4 3 2 1	4 3 1 2	3 4 2 1	1 2 3 4	1 4	1 2 3 4	1 2 3	2 1 3
0.50	3 4 2 1	3 4 1 2	4 1 2 3	3 2 1 4	1 3 2	1 4 3	1 3 2 4	1 2 3	1 2 3 4
0.45	3 4 1 2	3 4 1 2	2	1 2 3 4	1 3	1 3 4	1 4 3 2	1 4 2 3	1 2 3 4
0.40	3 1	1 2 3	2 1 3	1 2 3	1 4 2	1 3 2 4	1 2 4 3	1 2 4 3	1 2 3 4
0.35	2 1	2 1	2 1 3	1 2 4	1 2 4	1 2 4	1 2 3 4	1 2 3 4	1 2 3 4
0.30	2 4	2 1	1 2	1 2 3 4	1 3 2	1 2	1 2 3 4	1 2 3 4	1 2 3 4
0.25	2	1 2	1 2	1 2	1 3 4 2	1 2 3 4	1 2 3 4	1 2 3 4	1 2 3 4
0.20	stable	1	1 2	1 3	1 2 4	1 2 3 4	1 2 3 4	1 2 3 4	1 2 3 4
0.15	stable	1 2	1	1 2 3	1 2 3	1 2 3 4	1 2	1 2 3	1 2 3
0.10	stable	1 2	1 2	1 2 3	1 2 3	1 2 3 4	1 2 3	1 2 3	1 2 3
0.05	stable	1	1	1	1 2	1 2	1	1	1 2 3

Table 4.2.2. Approximate modal dominance regimes for $q = 1.75$ and 2.0 for $m = 1, 2, 3$, and 4.

Instability Regimes:

For large star mass, *Kepler* disks (q = 1.5) are stable while q = 2 (constant specific angular momentum disks are unstable (Papaloizou & Pringle 1984). We find that *Kepler* disks are unstable for even fairly massive stars (Hadley & Imamura 2009,2011, Hadley *et al.* 2011).

Nonlinear simulations are needed to determine the outcome of instability. Complicating the problem is that multiple modes are generally unstable for a given disk model.

	q = 2.0								
0.65	4 3 2 1	4 3 2 1	4 3 2 1	4 2 3 1	4 3 2 1	3 4 1 2	1	1 3 2	2 3 1 4
0.60	4 3 2 1	4 3 2 1	4 3 1 2	3 4 2 1	3 2 4 1	1	1	1 2 4	2 1 4
0.55	4 3 2 1	4 3 2 1	4 3 1 2	3 4 2 1	1 2 3 4	1 4	1 2 3 4	1 2 3	2 1 3
0.50	3 4 2 1	3 4 1 2	4 1 2 3	3 2 1 4	1 3 2	1 4 3	1 3 2 4	1 2 3	1 2 3 4
0.45	3 4 1 2	3 4 1 2	2	1 2 3 4	1 3	1 3 4	1 4 3 2	1 4 2 3	1 2 3 4
0.40	3 1	1 2 3	2 1 3	1 2 3	1 4 2	1 3 2 4	1 2 4 3	1 2 4 3	1 2 3 4
0.35	2 1	2 1	2 1 3	1 2 4	1 2 4	1 2 4	1 2 3 4	1 2 3 4	1 2 3 4
0.30	2 4	2 1	1 2	1 2 3 4	1 3 2	1 2	1 2 3 4	1 2 3 4	1 2 3 4
0.25	2	1 2	1 2	1 2	1 3 4 2	1 2 3 4	1 2 3 4	1 2 3 4	1 2 3 4
0.20	stable	1	1 2	1 3	1 2 4	1 2 3 4	1 2 3 4	1 2 3 4	1 2 3 4
0.15	stable	1 2	1	1 2 3	1 2 3	1 2 3 4	1 2	1 2 3	1 2 3
0.10	stable	1 2	1 2	1 2 3	1 2 3	1 2 3 4	1 2 3	1 2 3	1 2 3
0.05	stable	1	1	1	1 2	1 2	1	1	1 2 3

Table 4.2.2. Approximate modal dominance regimes for q = 1.75 and 2.0 for m = 1, 2, 3, and 4.

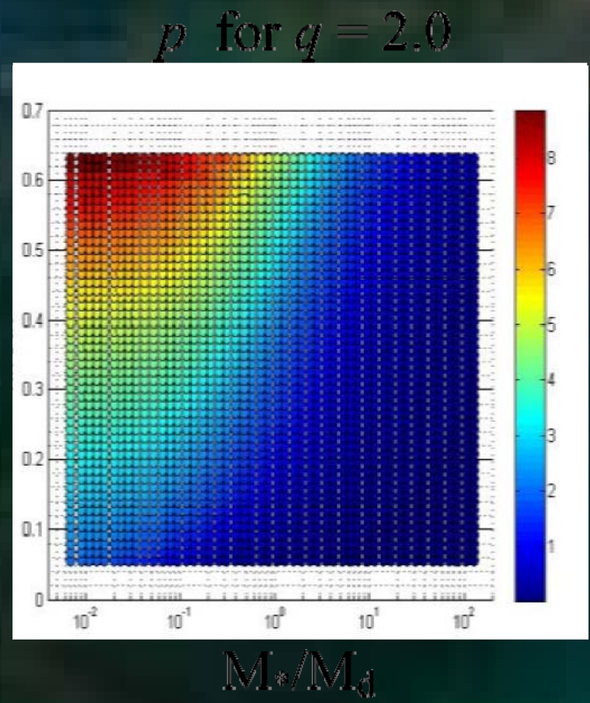

The parameter *P* was introduced by Christodoulou and Narayan (1992) as a measure of the importance of self-gravity to pressure. The shape of the constant *P*-curves in the R(in)/R(out)-Stellar Mass parameter space (right panel) roughly tracks where mode changes occur and serves as an interesting disk stability parameter. For *P* > 2.97, 5.205, and 7.526, I modes are unstable, J modes are unstable, and J modes dominate I modes for q=2 (see Christodoulou and Narayan 1992, Christodoulou 1993, Andalib, Tohline, and Christodoulou 1998). We find that the I mode threshold is *P* ~ 3.5 and J modes dominate I modes for *P* > 5.7 for q=2.

III. Angular Momentum Transport:

Quasi-linearTheory and Nonlinear Simulations

Conservation of Angular Momentum

$$\vec{f} = \frac{\partial}{\partial t}\rho\vec{v} = -\vec{\nabla}\cdot\overleftrightarrow{\mathrm{S}},$$

where $\vec{f}$ is the force density and $\overleftrightarrow{\mathrm{S}}$ is the Stress Tensor given by,

$$\overleftrightarrow{\mathrm{S}} = \rho\vec{v}\vec{v} + \overleftrightarrow{\Pi} + \frac{1}{8\pi G}\vec{\nabla}\Phi_g\vec{\nabla}\Phi_g$$

and $\overleftrightarrow{\Pi}$ is the pressure tensor. The torque density about the origin is then

$$\vec{\Upsilon} = \vec{r}\times\vec{f}$$

where $\vec{r}$ is the radial vector. The torque density about the z-axis is then

$$\Upsilon_z = -\frac{1}{s}\frac{\partial}{\partial s}(\delta\rho\delta v_s s v_\circ + \rho_\circ\delta v_s\delta v_\phi s) - \frac{\partial}{\partial z}(\rho_\circ\delta v_\phi\delta v_z + \delta\rho\delta v_\circ\delta v_z) - m\delta\rho\delta\Phi_g$$

We drop first order terms because they integrate to zero over azimuthal angle and a cycle. Nonlinear interaction terms survive averaging and may explain the early nonlinear behavior found in numerical simulations (see also Woodward *et al.* 1994, Laughlin *et al.* 1997,1998, Adams & Laughlin 2000, Imamura *et al.* 2000,2003).

Quasi-Linear Results:

Gravitational Self-Interaction torque

I^+

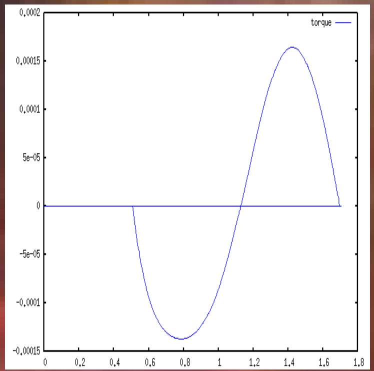

$q = 1.5,\ r_-/r_+ = 0.30\ M_*/M_d = 0.0$

I^-

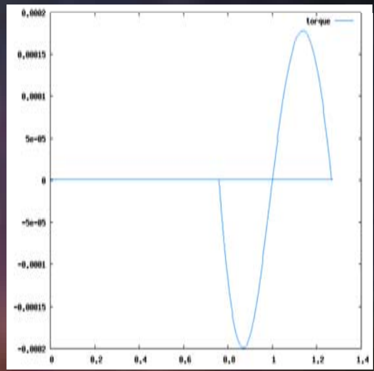

$q = 1.5,\ r_-/r_+ = 0.60\ M_*/M_d = 0.1$

J

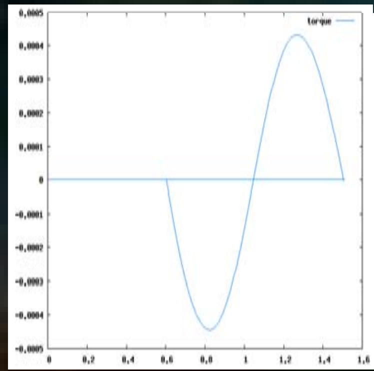

$q = 1.5,\ r_-/r_+ = 0.40\ M_*/M_d = 0.0$

P

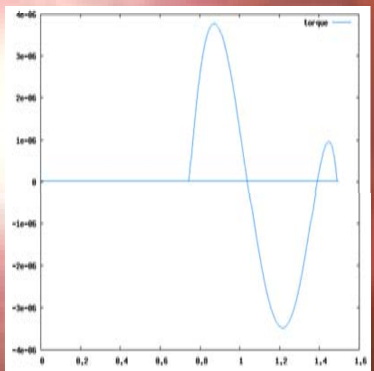

$q = 2.0,\ r_-/r_+ = 0.50\ M_*/M_d = 100.0$

Edge

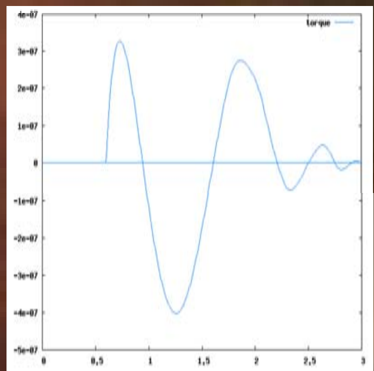

$q = 2.0,\ r_-/r_+ = 0.20\ M_*/M_d = 100.0$

A

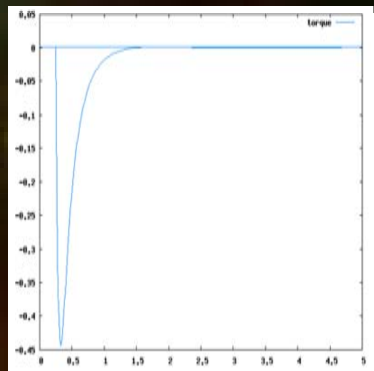

$q = 1.75,\ r_-/r_+ = 0.05\ M_*/M_d = 0.1$

Mode Evolution:

Angular momentum evolution

I^+

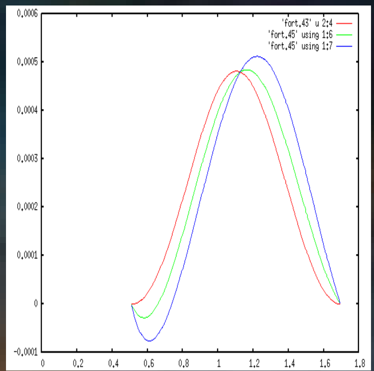

q = 1.5, r_-/r_+ = 0.30 M_*/M_d = 0.0

I^-

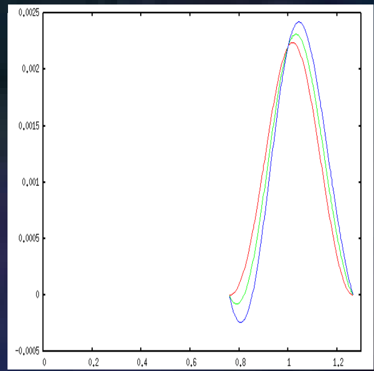

q = 1.5, r_-/r_+ = 0.60 M_*/M_d = 0.1

J

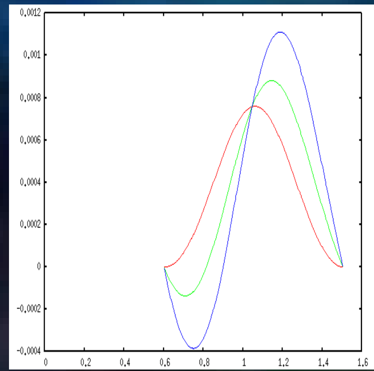

q = 1.5, r_-/r_+ = 0.40 M_*/M_d = 0.0

P

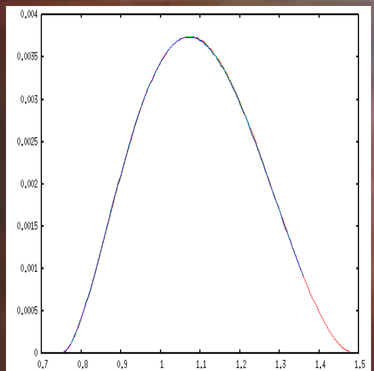

q = 2.0, r_-/r_+ = 0.50 M_*/M_d = 100.0

Edge

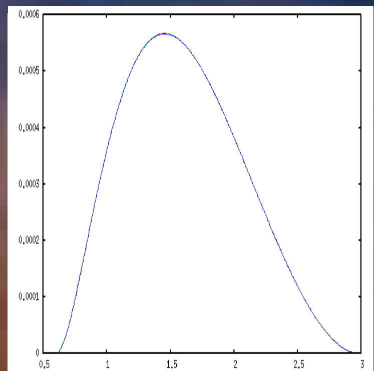

q = 2.0, r_-/r_+ = 0.20 M_*/M_d = 100.0

A

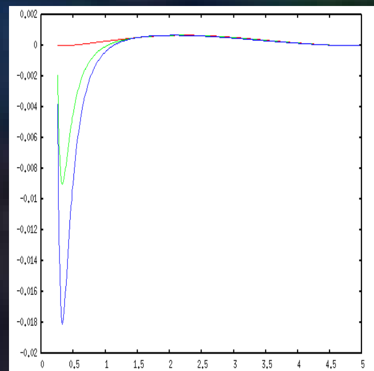

q = 1.75, r_-/r_+ = 0.05 M_*/M_d = 0.1

Nonlinear Results: Growth rates

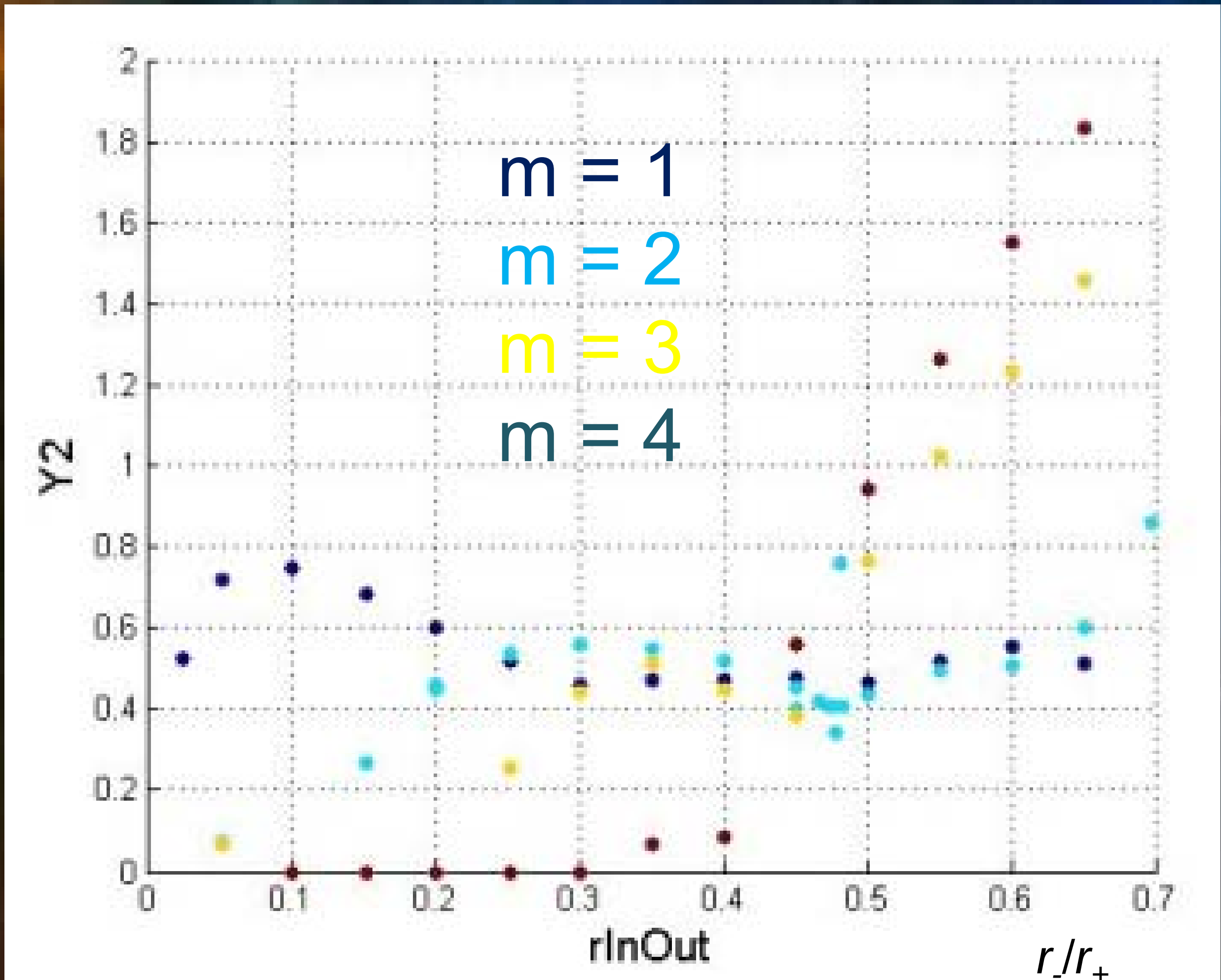

For star/disk systems, the situation is complex as several modes with similar growth rates may be unstable in given systems. Which mode dominates is then left to nonlinear simulations.

A. Nonlinear I^- mode

Time history of the Fourier Power of low m-modes

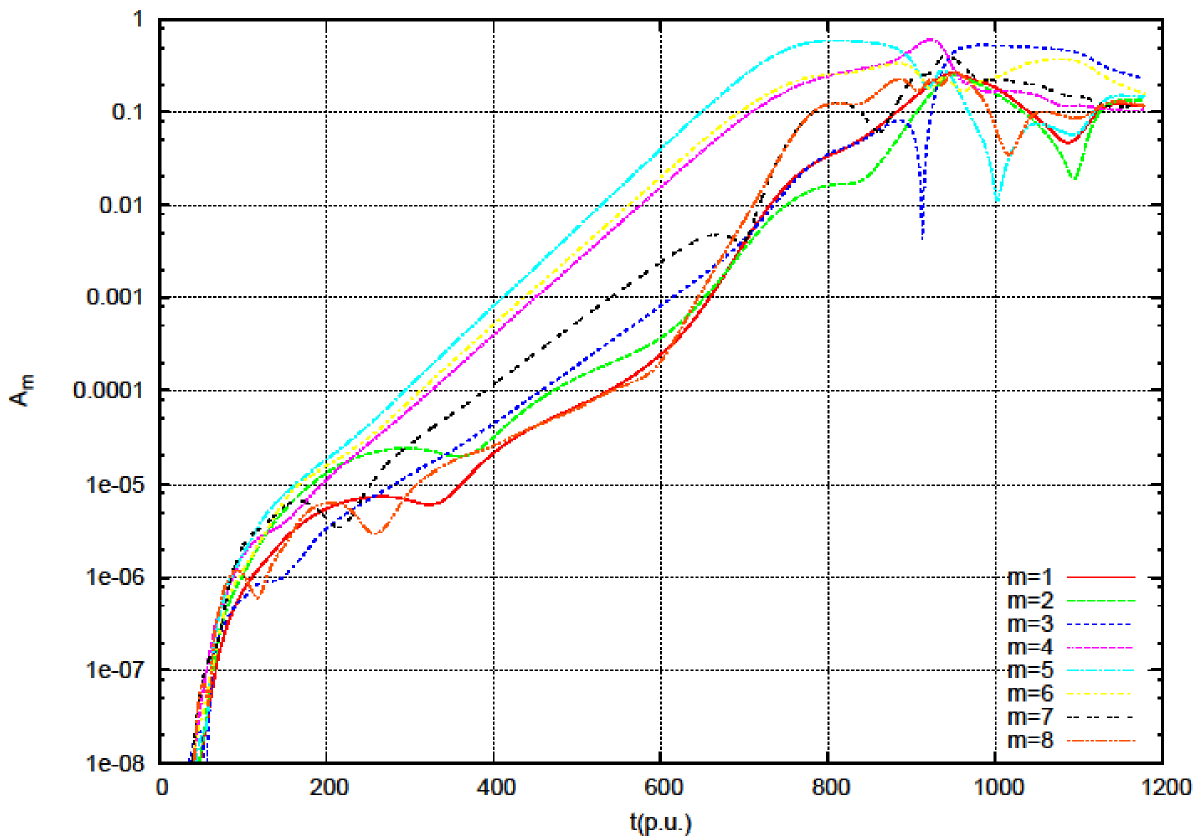

m	nonlinear	linear
1	0.7(?)	0.55
2	0.83(?)	0.50
3	1.19	1.24
4	1.48	1.55
5	1.64	1.58

System Parameters:

(n,q)=(1.5,1.5)
(M,m)=(0.1,1)
R(in)/R(out)=0.1
T/|W|=0.338
MIRP=510 p.u.

Nonlinear l^- model

Equatorial Plane Density Contour plots

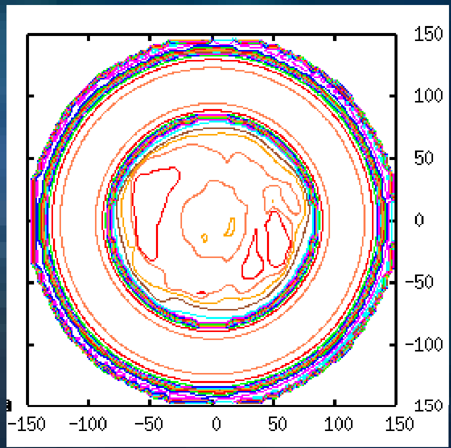

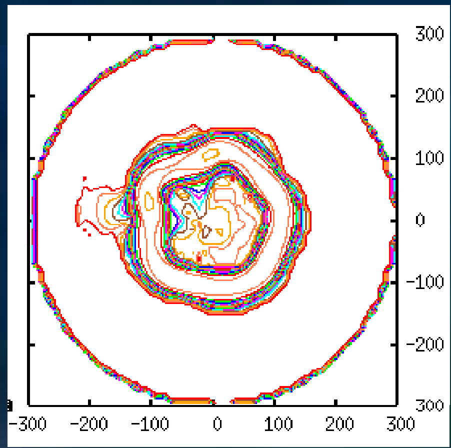

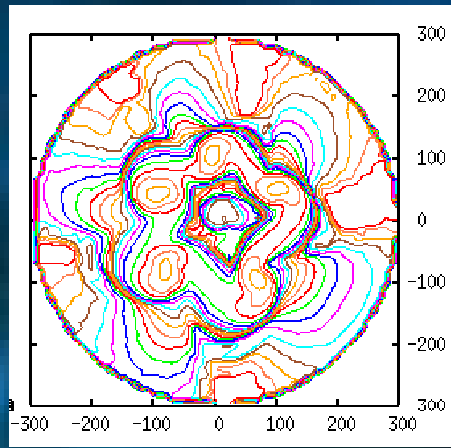

time

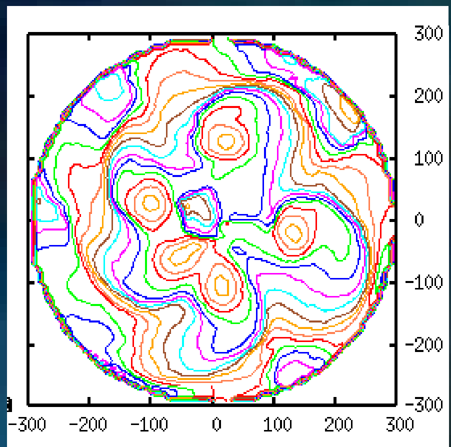

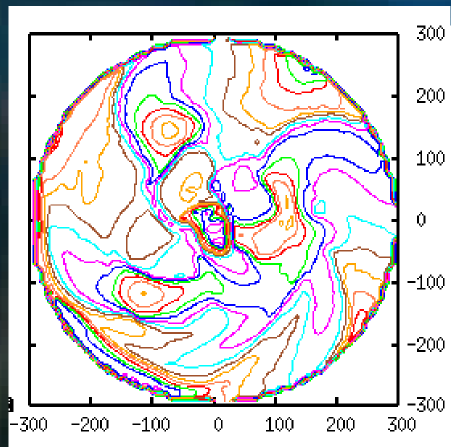

Nonlinear and linear l^{-} modes:

Eigenfunction phases in Equatorial Plane

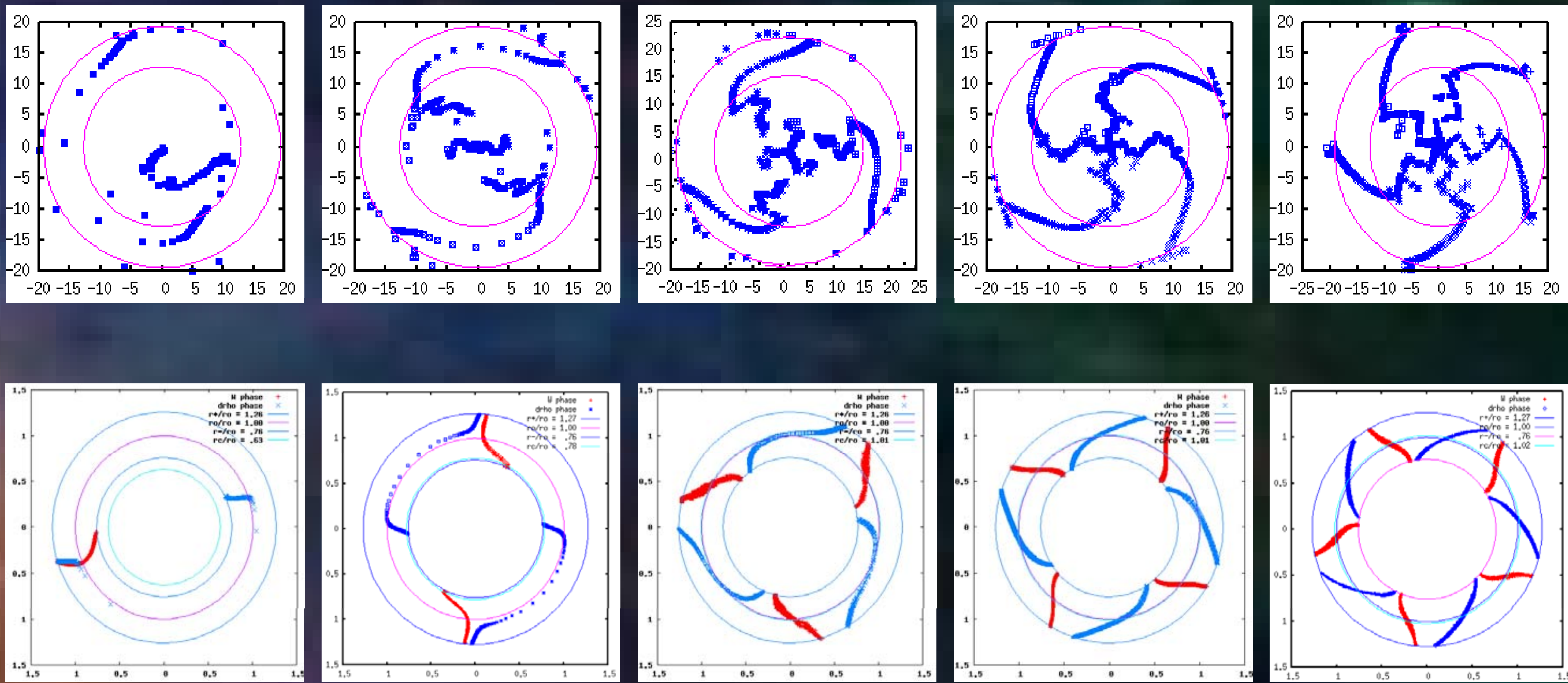

Nonlinear and linear l⁻ modes:

Eigenfunction amplitudes in Equatorial Plane

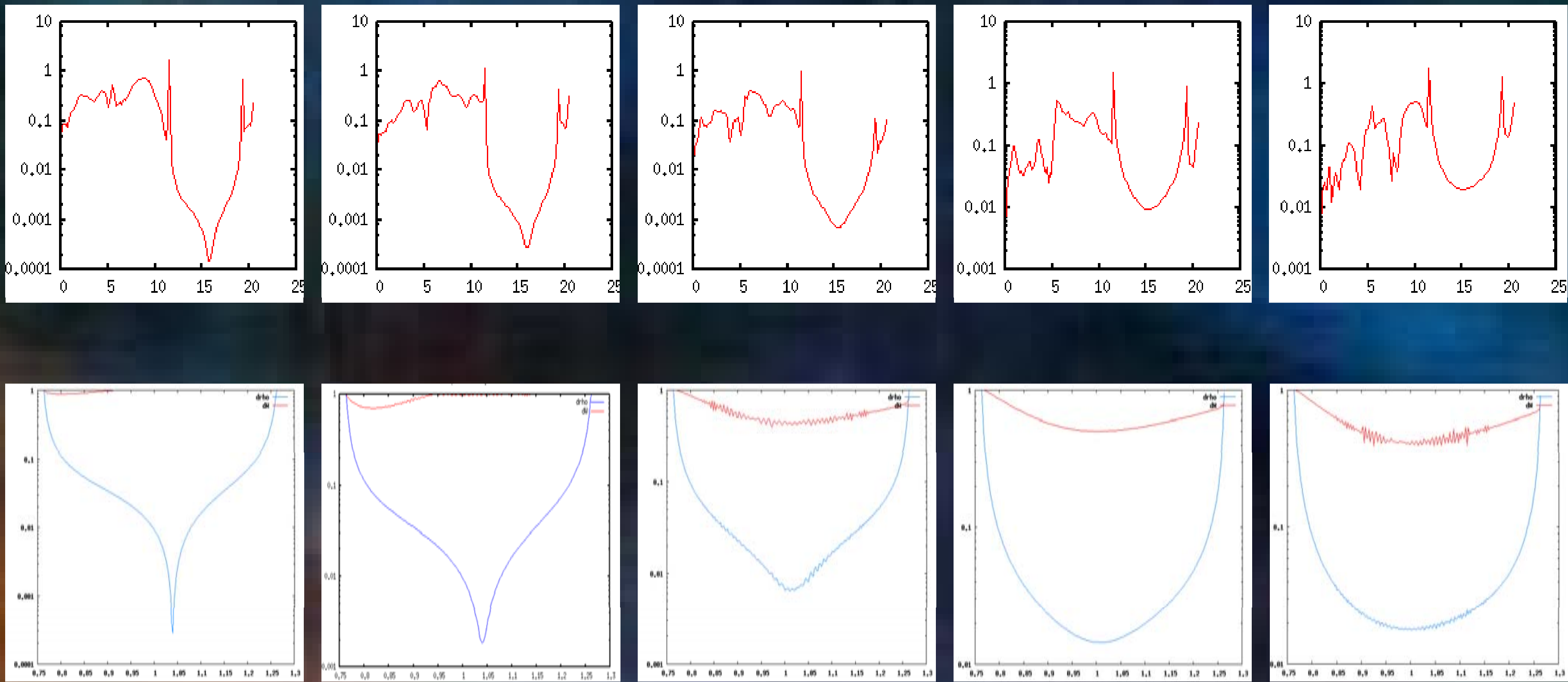

Comparison of QL and NL torques

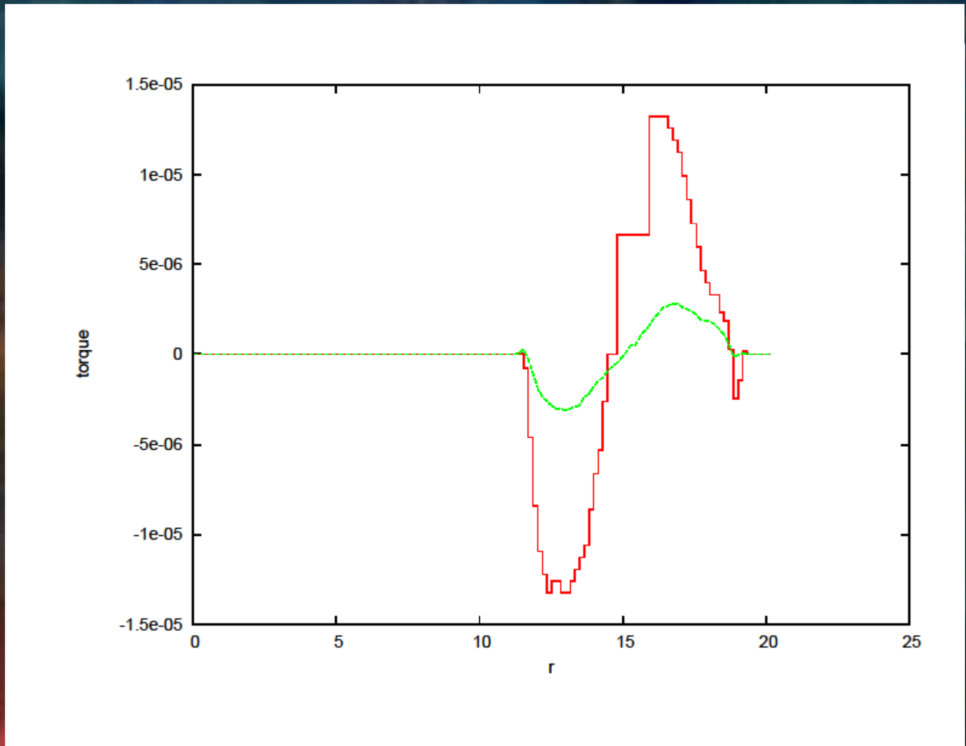

The total torque (red curve) and advective torque (green curve) for the nonlinear simulation when the m = 5 density perturbation's amplitude ~ 0.01.

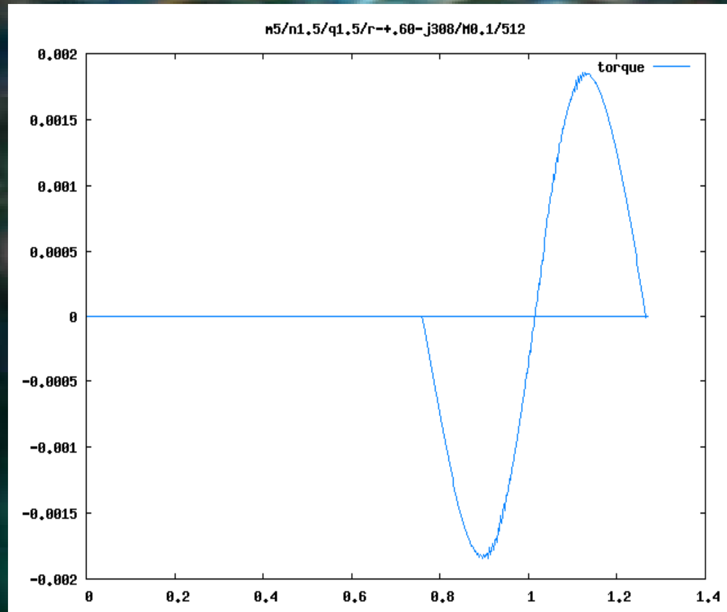

The quasi-linear gravitational self-interaction torque for the m = 5 mode. The torque is calculated for the normalization that the density perturbation integrated over the disk volume is 1.

Evolution of the Mass and Angular Momentum Distributions

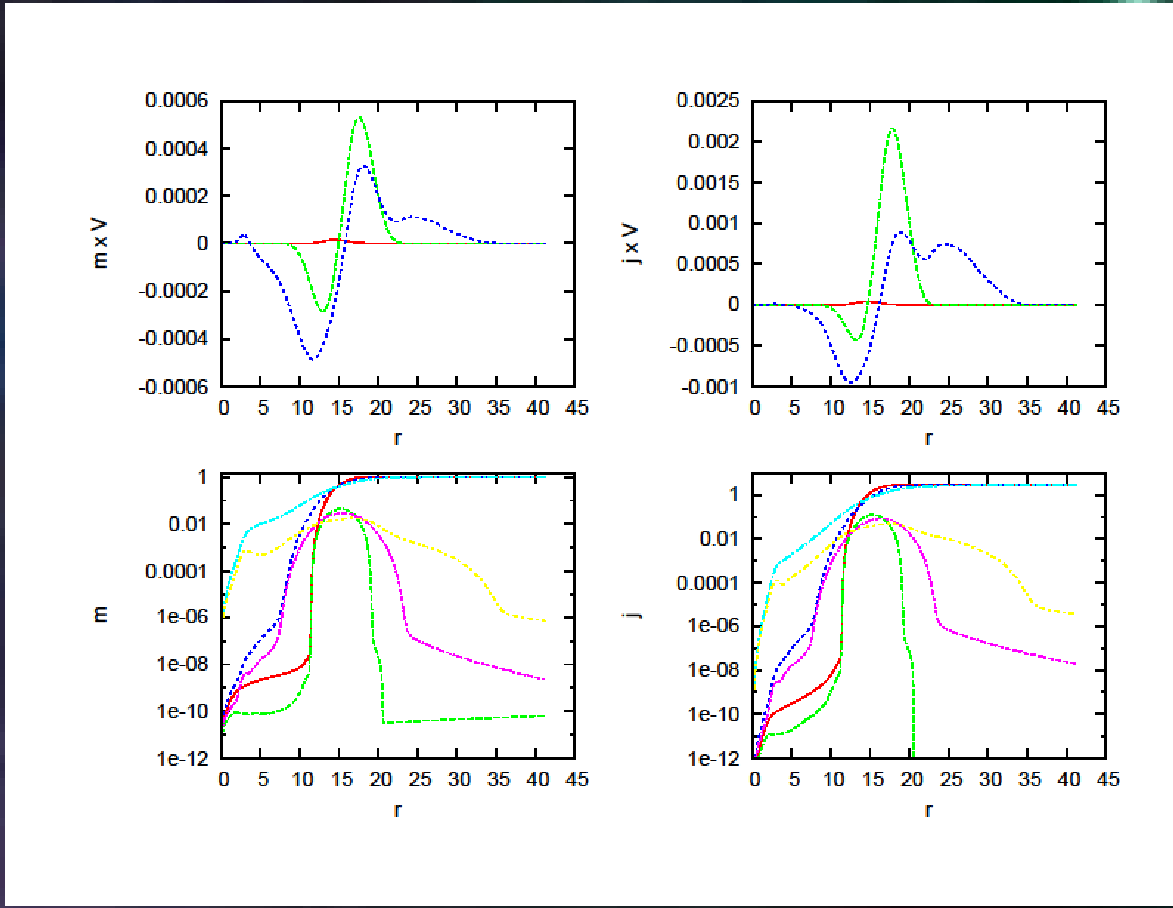

The mass distribution is on the left and the angular momentum distribution is on the right. The times presented are 525 p.u. (1.03 Mirps, red), 712 p.u. (1.49 Mirps, green), and 836 p.u. (1.64 Mirps, blue).

B. Nonlinear P mode:

Time history of the Fourier Power of low m-modes

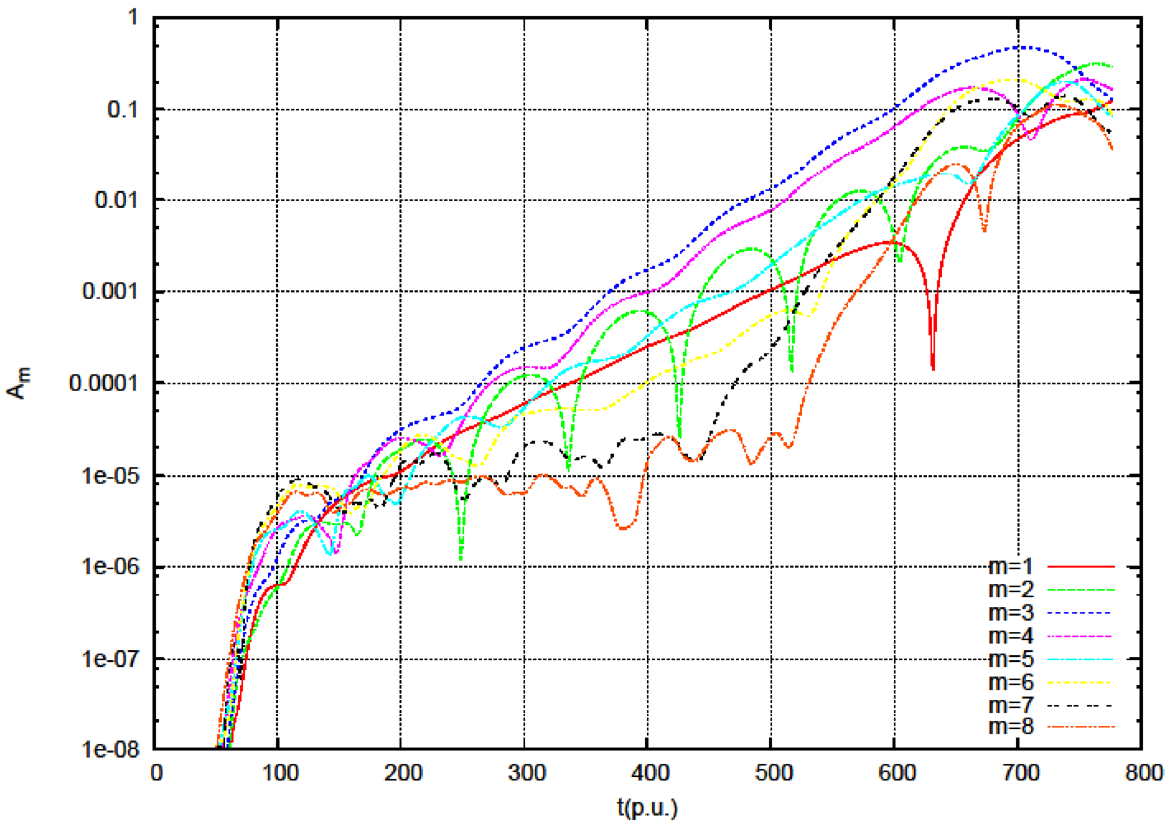

m	nonlinear	linear
1	….	…..
2	0.39	…
3	0.47	0.431
4	0.47	0.449
5	0.39	0.362

System Parameters

(n,q)=(1.5,2)
(M,m)=(5,1)
R(in)/R(out)=0..661
T/|W|=0.471
MIRP=140 p.u.

Nonlinear P modes:

Equatorial Plane Density Contour plots

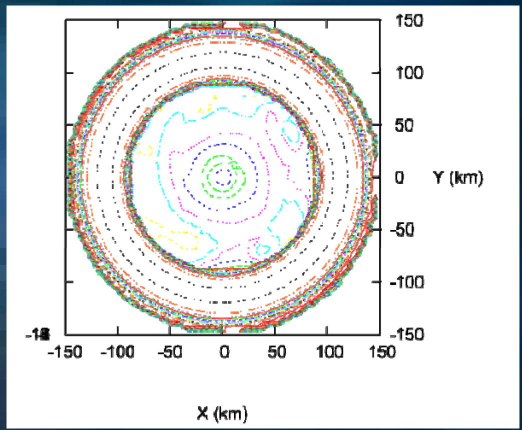

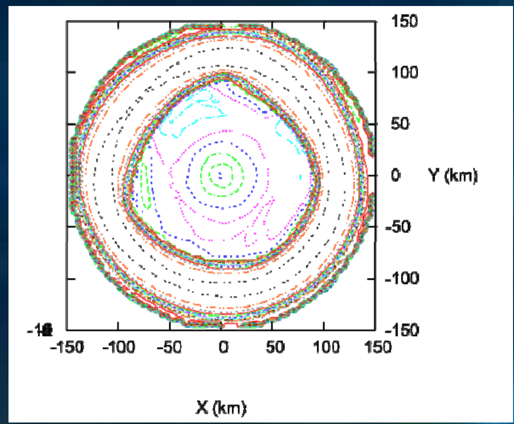

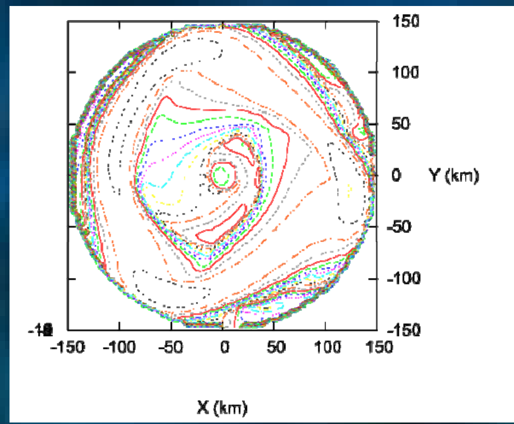

time

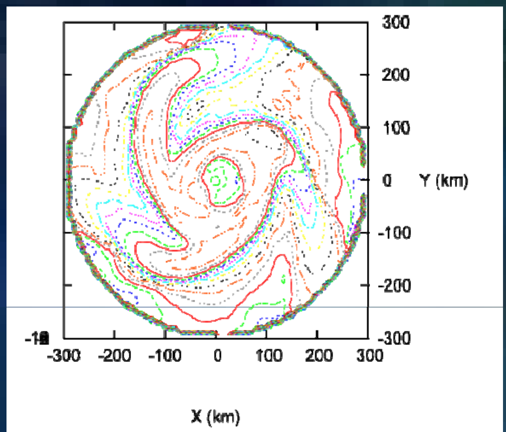

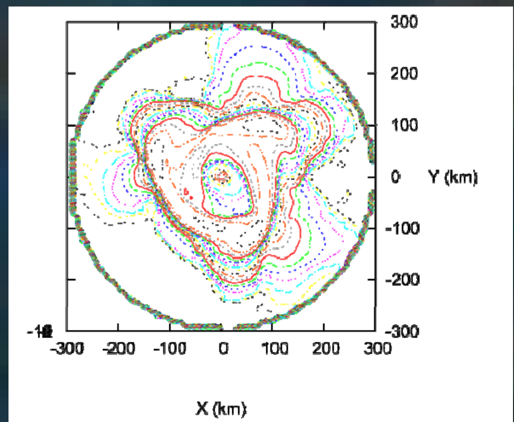

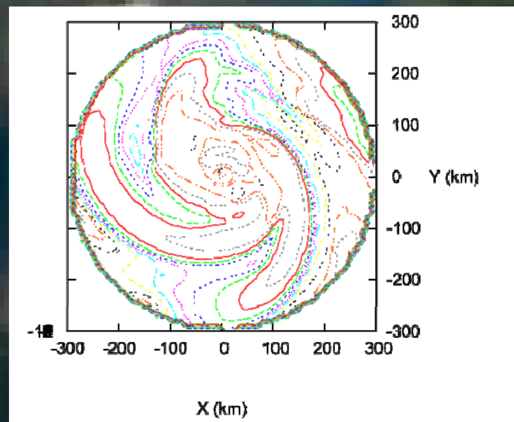

Nonlinear and linear P modes:

m = 3 mode Eigenfunctions in Equatorial Plane

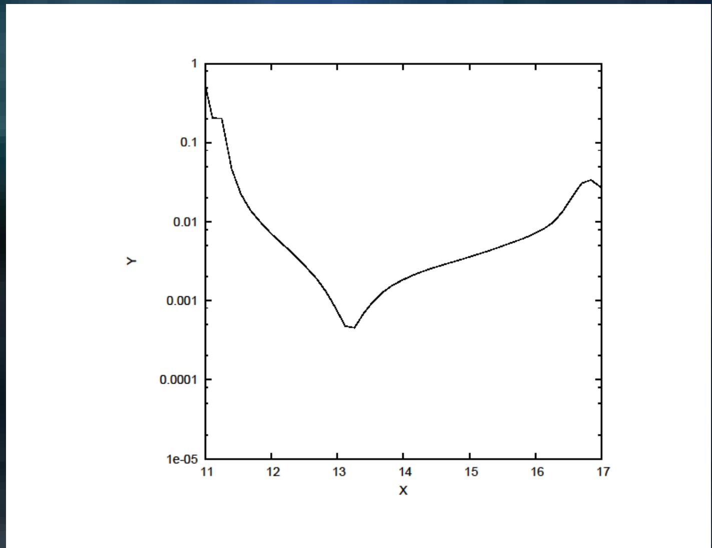

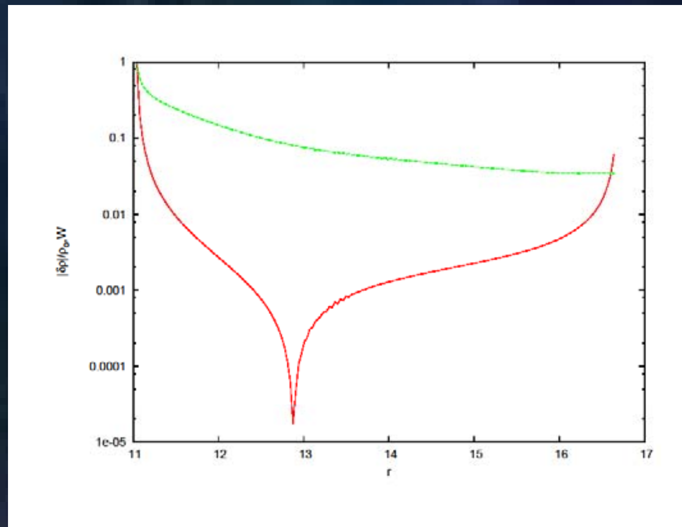

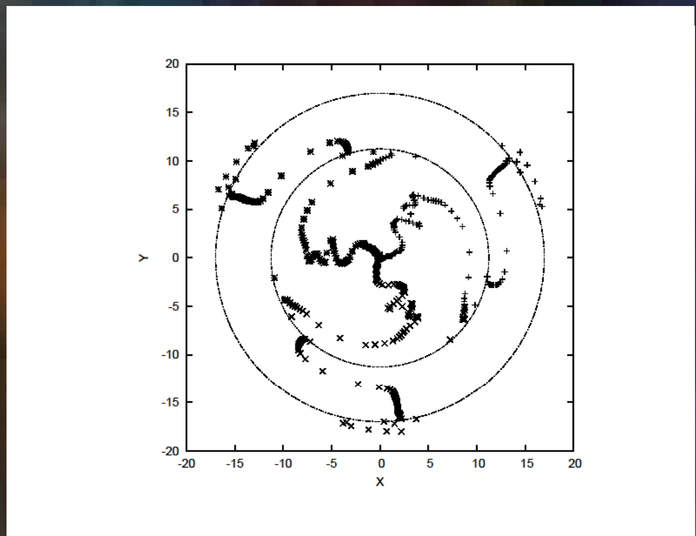

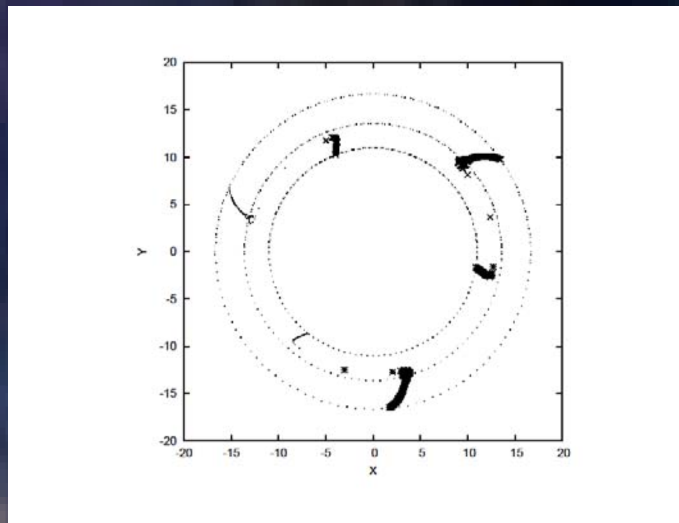

Comparison of QL and NL P Mode Torques

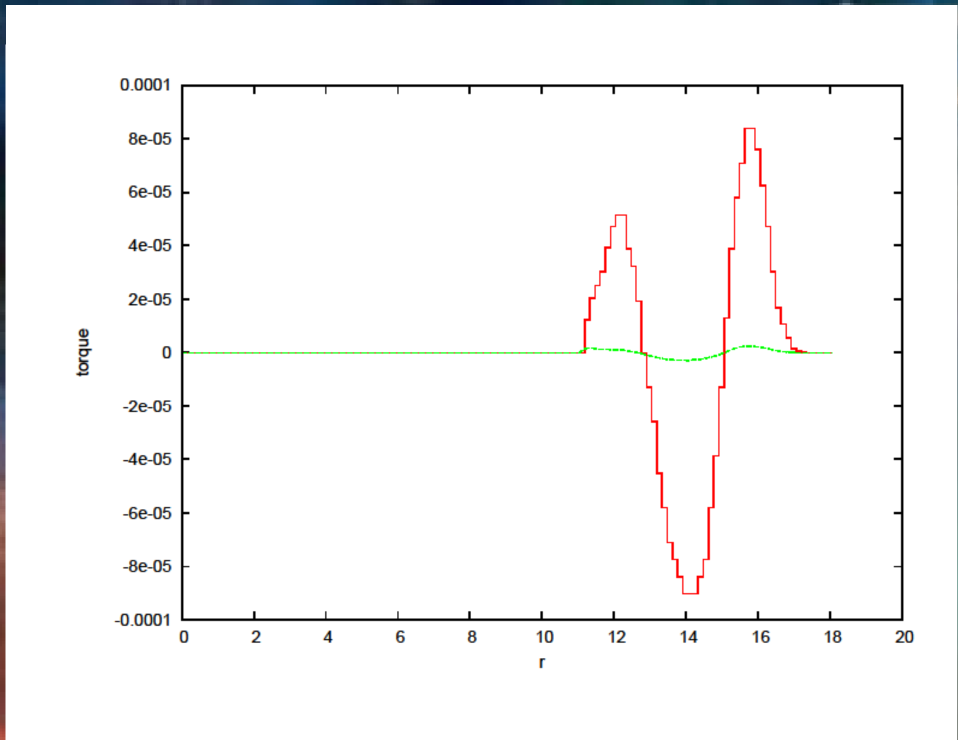

The total torque (red curve) and *advective torque* (green curve) for the nonlinear simulation when the m = 3 density perturbation's amplitude ~ 0.0019.

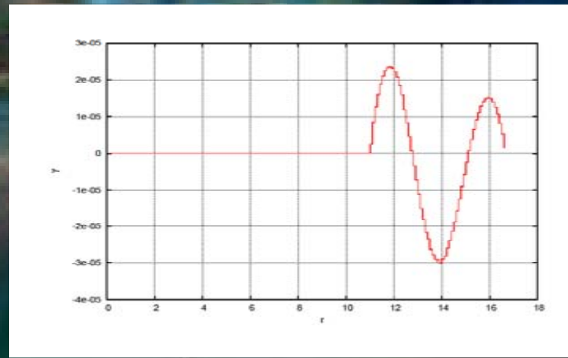

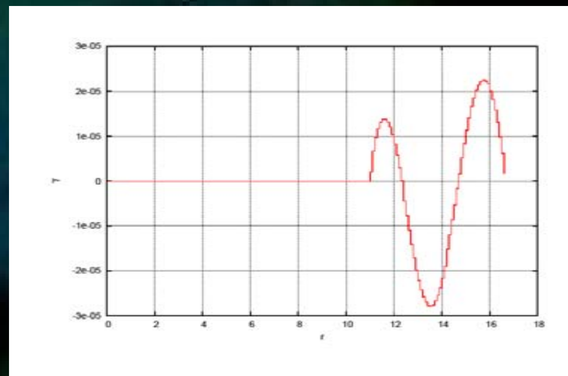

The quasi-linear gravitational self-interaction torque for the m = 3 and 4 modes. The torques are calculated for the normalization in which the density perturbation integrated over the disk volume is 1.

Evolution of the Mass and Angular Momentum Distributions

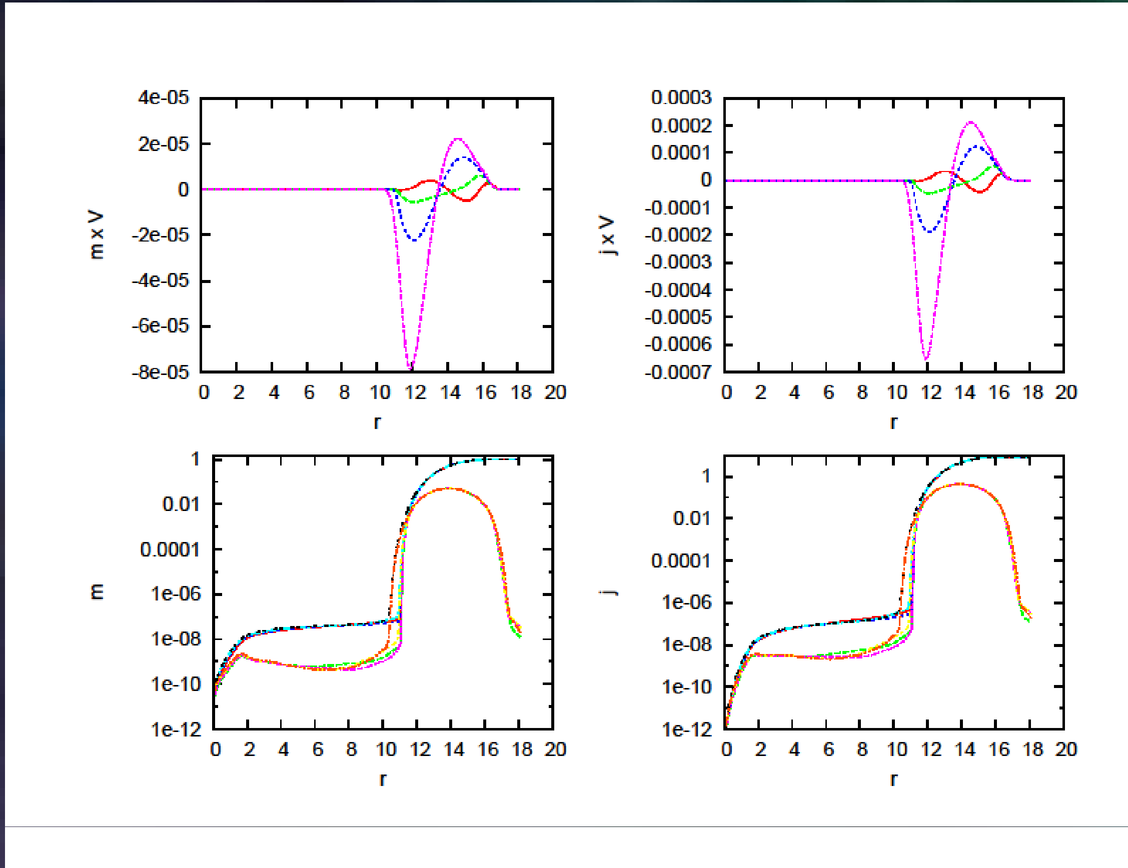

The mass distribution is on the left and the angular momentum distribution is on the right. The times presented are 405 p.u. (2.89 Mirps, red), 463 p.u. (3.30 Mirps, green), 523 p.u. (3.73 Mirps, blue), and 574 p.u. (4.10 Mirps,magenta)

IV. Summary and Future Directions

- Performed linear, quasi-linear, and non-linear modeling of massive, self-gravitating disks
- Massive, self-gravitating disks are unstable over large parts of parameter space
- Quasi-linear analysis yields good predictions of the early nonlinear behavior of linearly unstable disks and leads to predictions of mass and angular momentum transport rates without resort to fully nonlinear calculations
- Saturation mechanisms and Supercritical Stability?
- Loosen assumptions for future work; include radiation in the nonlinear regime, include magnetic fields, include realistic equation-of-state

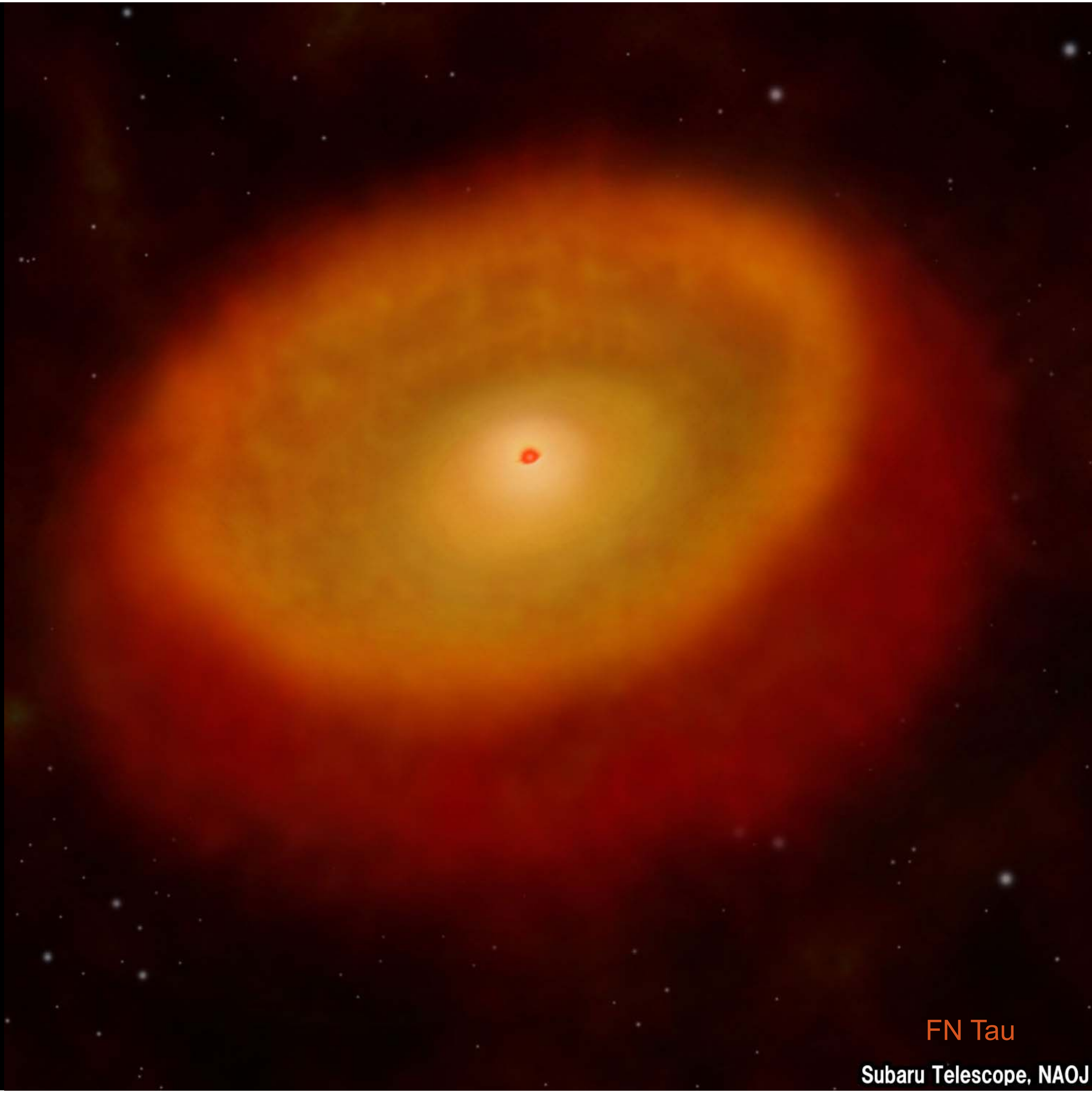
FN Tau
Subaru Telescope, NAOJ